An Isoperibol Calorimeter for the Investigation of Biochemical Kinetics and Isothermal
Titration Calorimetry

By

Ovid Charles Amadi

SUBMITTED TO THE DEPARTMENT OF MECHANICAL ENGINEERING IN
PARTIAL FULFILLMENT OF THE REQUIREMENTS FOR THE DEGREE OF

BACHELOR OF SCIENCE
AT THE
MASSACHUSETTS INSTITUTE OF TECHNOLOGY
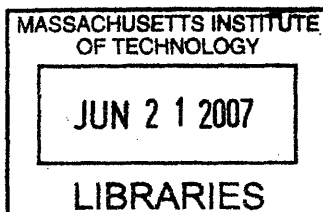

JUNE 2007

Signature of Author:_____
Department of Mechanical Engineering
May 11, 2007

Certified by:_____
Ian W. Hunter
Professor of Mechanical Engineering
Thesis Supervisor

Accepted by:_____
John H. Lienhard V
Professor of Mechanical Engineering
Chairman, Undergraduate Thesis Committee

1

An Isoperibol Calorimeter for the Investigation of Biochemical Kinetics and Isothermal Titration Calorimetry

by

Ovid Charles Amadi

ABSTRACT

Isothermal titration calorimetry is a technique used to measure the enthalpy change associated with a molecular binding interaction. From these data, the binding constant for the reaction can be determined. In the scope of a larger project to design a high sensitivity instrument for collecting such data, the current methods in isothermal titration calorimetry were investigated. Further calorimetric experience was acquired by designing a large scale calorimetric device. Dilution reactions with dimethyl sulfoxide and water were conducted to measure the excess enthalpy of binding. The inaccuracy of these measurements necessitated the more careful design of an isoperibol calorimeter. This calorimeter was modeled was an arrangement of coupled thermal masses and capacitances in order to fully understand its transient response to a thermal input. Dilution reactions and a neutralization reaction with HCl and NH_4OH were performed on the system and the results were used to make recommendations for the design of the future high sensitivity device.

Table of Contents

Introduction

In order to design and construct and accurate and highly sensitive nano-calorimeter for detecting the heat produced by biological reactions, it is necessary that both the biochemical and thermodynamic situations are fully understood. To achieve this goal, the enzyme kinetics and calorimetric techniques were analyzed in parallel. The result is captured by this document which first serves to outline the basic principles that describe the biological and chemical interactions that underline biocalorimetric processes, particularly that of isothermal titration calorimetry (ITC). The discussion will begin with a description of the thermodynamic and kinetic characteristics of enzyme catalyzed reactions and the key observations that render biocalorimetry an applicable measurement technique before reporting on the analyses and experiments that were employed to better understand biocalorimetry.

Enzyme Binding and Kinetics

Reaction Rates and Rate Laws

Rate constants are used to relate the concentration of reactants to the reaction rate of a chemical reaction. The reaction rate is the time derivative of the product concentration and is proportional to the rate constant and powers of the concentrations of the reactants. A chemical reaction with a general stoichiometric relationship given by $aA + bB \rightarrow C$ and a rate constant, k, will have a reaction rate, r, give by:

$$r = k[A]^a [B]^b, \tag{1}$$

where the bracket notation indicates concentration. An equation of the form shown in Equation. 1 is called a rate law and its order is given by the sum of the exponents of the concentration factors (in this case the sum of a and b). By definition the reaction rate must have units of concentration per unit time, thus the units of k depend on the order of the rate law.

Single step enzyme catalyzed reactions are composed of two distinct in-series steps. The first is the binding of the substrate (S) to the enzyme (E) to produce the enzyme-substrate complex (ES). During the second step, the substrate is converted into the reaction product (P) and the enzyme is reverted back to its free state. Both these reactions can proceed in the reverse direction and are thus reversible. The overall reaction with rate constants, k_1 and k_{-1} representing the forward and reverse rate constants for the enzyme-substrate complex formation and k_2 and k_{-2} representing the forward and reverse rate constants for the free enzyme and product formation, is given by:

$$E + S \underset{k_{-1}}{\overset{k_1}{\longleftrightarrow}} ES \underset{k_{-2}}{\overset{k_2}{\longleftrightarrow}} E + P. \tag{2}$$

Michaelis-Menten Kinetics

The above mechanism wherein the enzyme catalyzed reaction is composed of two successive steps, the first much faster than the second, was first suggested by Leonor Michaelis and Maud Menten in 1913. This model has been used to formulate an expression for the initial rate or velocity of the reaction. This quantity is used to generally describe the kinetics of the reaction. Experimentally, it has been shown that the initial velocity (V_0) will at first increase linearly with increasing substrate concentration, but will eventually plateau at a maximum value (V_{max}) as shown in Figure. 1.
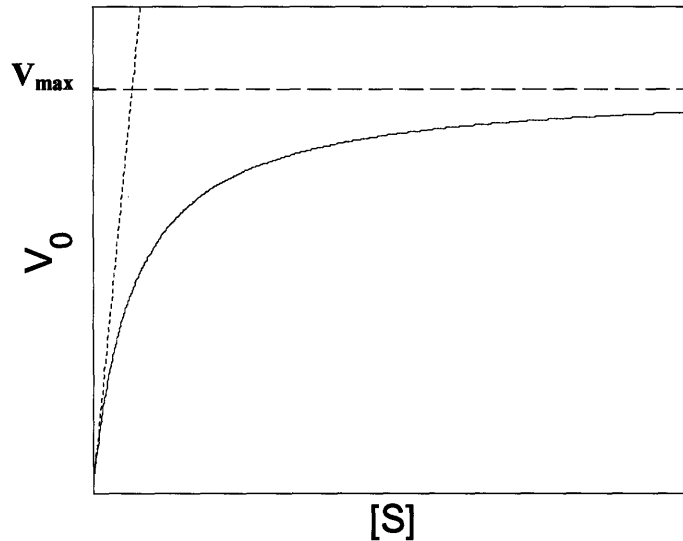
Figure 1: Illustrates the dependence of initial velocity [concentration/time] on substrate concentration. Initially the initial velocity increases linearly with increasing substrate, as indicated by the dotted line in the figure, but eventually saturates to the maximum velocity, dashed line, at high substrate concentration values.

Both experimentally and in practice, the concentration of the substrate is often much larger than the concentration of the enzyme. Thus during the course of the reaction, particularly the first several seconds, the concentration of the substrate changes very little and so, as shown above, the initial velocity may be considered a function of substrate concentration. The conversion of ES to E and P is the slower step in the reaction and thus the rate-limiting step. The reaction rate is proportional to [ES] because the reaction cannot proceed any faster than ES is consumed. At low [S], there is an excess of E and equilibrium is pushed towards the formation of ES. Increases in [S] yield proportional increases in [ES]. However, when [S] is very large, nearly all E is converted to ES and additional increases in [S] will not produce significant increases in [ES], in this case the ES state is saturated and the initial velocity increases very slowly.

The development of an analytical description of enzyme kinetics includes a steady state assumption suggested by Briggs and Haldane in 1925. When an enzyme catalyzed reaction begins, [ES] is zero. Initially, there exists a period, typically lasting microseconds, where [ES] increases to a steady state value. After this period, [ES] does not change and the reaction rate that is measured thereafter is the initial velocity.

Moreover, during the initial stages of the reaction, [P] is very low and the reverse of its formation can be considered negligible. This simplifies the expression for the initial velocity which now depends only on [ES],

$$V_0 = k_2[ES].$$ (3)

An expression for [ES] is found by equating the rate of formation of ES with the rate of disappearance of ES, by virtue of the steady state assumption, and noting that [E], representing the amount of free enzyme at any time, is equal to the total amount of enzyme, [E_t], less the amount of bound enzyme. Here the concentration of the substrate is considered constant as it is much larger than the enzyme concentration and does not change appreciably,

$$[ES] = \frac{[E_t][S]}{[S] + \frac{(k_2 + k_{-1})}{k_1}}.$$ (4)

The product of [ES] and k_2 gives the initial velocity. Substituting the Michaelis constant, K_m, for $(k_2 + k_{-1})/k_1$ and recognizing that V_{max} occurs when all the enzyme is in the ES form yields the Michaelis-Menten equation which captures the contributions to the initial velocity of the reaction,

$$V_0 = \frac{V_{max}[S]}{K_m + [S]}.$$ (5)

Binding Constant

Once the binding step of the enzyme catalyzed reaction begins, enzyme and substrate bind reversibly until the steady state equilibrium concentrations exist. In this state, the concentrations of free enzyme, substrate, and bound enzyme do not change. This is the case with all chemical reactions in a closed system - at equilibrium the rate of product formation is equal to the rate at which product is converted back to reactants. For a generalized reaction of the form $aA + bB \leftrightarrow cC + dD$, with a forward and reverse rate constants of k_f and k_r, respectively, at equilibrium:

$$k_f [A]^a [B]^b = k_r [C]^c [D]^d .\tag{6}$$

Rearranging Equation 6 produces an expression for a constant known as the equilibrium constant, K_{eq}, which relates the relative concentrations of products and reactants at equilibrium,

$$\frac{[C]^c [D]^d}{[A]^a [B]^b} = \frac{k_f}{k_r} = \text{a constant} = K_{eq} .\tag{7}$$

When the equilibrium constant is large (greater than unity), the concentration of the products are generally larger than that of the reactants and the reaction tends toward the creation of product. In the opposite case, when the equilibrium constant is less than unity, the reaction tends toward the creation of the reactants.

With respect to the enzyme binding reaction, $E + S \leftrightarrow ES$, the equilibrium constant may be referred to as the binding constant The binding constant, K_b, describes the equilibrium concentrations of free enzyme, free substrate, and bound enzyme:

$$K_b = \frac{[ES]}{[E][S]} .\tag{8}$$

This constant effectively measures the propensity of the enzyme to exist primarily in the bound or free state and is a measure of the affinity of the enzyme for the substrate. The dissociation constant, K_d, the reciprocal of the binding constant corresponds to the substrate concentration at which half of the total enzyme is in the bound state, that is, the amounts of free and bound substrate are equal. This can readily be shown by substituting $1/K_b$ for $[S]$ in Equation 8. Here still this assumes that the concentration of bound enzyme is much less than the substrate concentration.

Weak vs. Tight and Slow vs. Fast

The binding constant effectively measures how tightly an enzyme is able to bind a ligand, that is, the greater the binding constant, the greater the proportion of enzyme that will be in the bound state at equilibrium. In comparing the affinity of an enzyme for different ligands, the dissociation constant may be used to indicate the ligand concentration at which half of the total enzyme will be in the bound form. Dissociation constants may range from the nano-molar to molar concentrations, wherein the more tightly bound interactions require a smaller ligand concentration to saturate 50% of the total enzyme concentration.

While the affinity of an enzyme for a substrate is determined by the relative magnitude of the forward and reverse rate constants, the speed at which the reaction occurs depends on the magnitude of these rate constants. Equation 9 describes the rate of formation of bound enzyme during an enzyme binding reaction given the assumption that the substrate concentration far exceeds that of the enzyme,

$$\frac{d[ES]}{dt} = k_1([E_t] - [ES])[S] - k_{-1}[ES].$$

(9)

Solving this differential equation with the initial condition that there is no bound enzyme at the onset of the reaction yields an expression for [ES] as a function of time,

$$[ES] = \frac{K_b[E_t][S]}{K_b[S] + 1}(1 - \exp(-(k_1[S] + k_{-1})t)).$$

(10)

The time constant, τ, for this temporal behavior is given by:

$$\tau = \frac{1}{k_1[S] + k_{-1}}.$$

(11)

Both increases in the forward and reverse rate constants will decrease the time constant and increase the speed at which the reaction occurs. Relatively large rate constants will

9

produce a relatively fast reaction, while smaller rate constants will produce a slow reaction.

Enthalpy of Reaction

During a chemical reaction, chemical bonds are broken and formed. The net energy of these processes is released as heat. At constant temperature and pressure, this quantity of heat is the enthalpy of reaction [J/mol] and specifies the amount of heat released or absorbed per mole of product formed. The enthalpy of reaction provides a means for tracking the progress of a reaction. The rate of heat production is proportional to the rate of product formation, and the amount of heat produced is proportional to the amount of product formed. Most enzyme binding reactions are exothermic and involve the release of heat.

It should be noted that enthalpy refers specifically to the heat transfer experience by a system at constant temperature and pressure where the only work transfer experienced by the system is volume-expansion work. The first law of thermodynamics, Equation 12, describes the change in energy, ΔE, of a system as the difference between the heat transfer, ΔQ, into the system and work, ΔW, done by the system.

$$\Delta E = \Delta Q - \Delta W .$$
(12)

If the only work done by the system is the volume-expansion work of changing volume by ΔV subject to a constant pressure, P, then

$$\Delta W = P\Delta V .$$
(13)

Combining Equations 12 and 13 and solving for ΔQ yields the heat transfer that accompanies a constant pressure volumetric expansion which is defined as the change in enthalpy ΔH,

$$\Delta H \equiv \Delta Q = \Delta E + P\Delta V. \tag{14}$$

Enthalpy can be used to calculate the Gibb's free energy of a system, which is the maximum amount of useful work that can be done by a system at constant temperature and pressure. Useful work is defined as work during a reversible process besides volume-expansion work. If the system in Equation 13 experiences a heat transfer in addition to the volumetric expansion then the remaining energy in the system, $\Delta H - \Delta Q_{rev}$, which can be used to go work is the change Gibb's free energy, ΔG. The second law of thermodynamics defines the change in entropy, ΔS, of a system as

$$\Delta S = \int \frac{\delta Q}{T} + S_{gen}, \tag{14}$$

where δQ is the heat transfer of the system at temperature T and S_{gen} is the entropy generated during the process. If the process is reversible and at a constant temperature then ΔS is the ratio of ΔQ_{rev} and T. And so,

$$\Delta H - \Delta Q_{rev} = \Delta E + P\Delta V - T\Delta S \equiv \Delta G. \tag{15}$$

Isothermal Titration Calorimetry

Setup and Procedure

Isothermal titration calorimetry (ITC) is a technique that may be employed to determine the equilibrium behavior of enzyme-substrate and general ligand-binding interactions. While more than a single method and instrument have been developed based on the principles of ITC, the subject of this section will focus on one of the more modern and popular approaches.

The ITC setup consists of two separate identical cells contained in a single adiabatic chamber. One cell is the reference cell wherein no reaction takes place, and the second is the reaction cell. For the case of a ligand binding to a protein, the reaction cell contains a known concentration and volume of the protein. A syringe, containing a known concentration of the ligand, is inserted into the reaction cell. Before beginning the experiment, the desired reaction temperature must be specified. Both the reference cell and the reaction cell will remain at this temperature for the duration of the experiment. The temperature of the adiabatic chamber may be set to a temperature below the reaction temperature such that heat must always be added to the two cells in order to keep them both at the reaction temperature.

The overall approach of ITC is to inject quantities of the ligand into the reaction cell. Prior to any injections a known amount of baseline power is continuously dissipated into the reaction cell such that it remains at the reaction temperature. After each ligand injection, as the reaction occurs, a quantity of heat is released proportional to the enthalpy of reaction. This heat would tend to increase the temperature of the reaction cell; however, the ITC instrument decreases the heat input to the reaction cell to keep the temperature difference between the reaction cell and the reference cell equal to zero. The output of the ITC instrument is the power input to the reaction cell as a function of time. After the injection, the reaction will proceed to equilibrium and no additional heat will be produced by the reaction and the power input will return to its baseline value, while the temperature difference between the cells continues to be zero. At this point, the next injection may take place and the process repeats itself.

The first ligand injection is smaller than the subsequent injections. This is done in order to eliminate the effects of any diffusion that may have occurred between the ligand solution and the protein solution, as well as to remove any air that may have been trapped at the tip of the syringe. As the ligand concentration in the reaction cell increases with subsequent injections the binding sites on the protein become saturated and additional ligand injections do not produce any heat due to the binding of ligand to the protein.

Analysis

<u>Heat of Dilution</u>

When a pure solute is dissolved in a pure solvent, the formation of solvent-solute interactions energetically competes with the disruption of the solute-solute and solvent-solvent interactions, and the result is a change in energy of the system by way of a heat transfer. The excess molar enthalpy of mixing for a solution is defined as the change in enthalpy that occurs when 1 mole of the solution is formed from its pure components. Suppose a solution of molality, m_1, is created by mixing a certain amount of a solute and solvent, and a second solution of molality, $m_2 > m_1$, is created by mixing the same amount of solute with a smaller amount of solvent. If the enthalpy of mixing for these two substances is exothermic, the heat of solution associated with the first solution will be greater in magnitude than that of the second solution because additional solute-solvent interactions occur in the former case. If additional pure solvent is added to the second solution until its molality is equal to m_1, the heat released by this process will be equal to the difference between the initial enthalpies of mixing for solutions 1 and 2. The heat released by this dilution of solution 2 is the heat of dilution between molalities m_2 and m_1.

During the ITC process relatively small volumes of the ligand solution are added to relatively large volumes of the protein solution. This is the equivalent of diluting the ligand solution through the addition of a large amount of solvent. With each injection, dilution of the ligand solution occurs and additional heat, corresponding to the heat of dilution between the ligand concentration in the syringe and the ligand concentration in the reaction cell, is released. This enthalpy change does originate from the binding of the ligand to the protein and must be removed from the ITC data. In order to quantify the heat of ligand dilution, the ITC procedure is performed a second time except the protein solution in the reaction cell is replaced by its buffer solution alone. The ITC data collected at each injection of this control process corresponds to the heat of ligand dilution in the experimental process.

In a similar fashion to the dilution of the ligand solution, with each injection the concentration of the protein solution changes as well. The volumes of ligand solution added to the reaction cell are much smaller than the volume of the protein solution, so the degree of dilution protein, and hence the heat of protein dilution are less than those of the ligand. However, a second control procedure must occur wherein the buffer solution without the ligand is titrated into the protein solution. The data collected at each injection of this second control process corresponds to the heat of protein dilution during the experimental process.

To ensure the accuracy of the ITC measurements, a final control process known as the machine blank must be executed. In this setup, buffer solution in the syringe is titrated into buffer solution in the reaction cell. The heat generated in this process accounts for any artifacts of the instrument during the ITC process (such as pressure changes) and is normally very small.

The final heat of interaction for the actual binding event is found by subtracting the heat of ligand dilution and heat of protein dilution from the ligand-protein ITC data at each injection and then adding in the heats from the machine blank procedure. The heats associated with the machine blank must be added into the calculation because they are doubly accounted for in the heats of ligand and protein dilution.

Buffer

The heats of dilution discussed above must be kept as low as possible so as to not create heats of dilution that mask the heat of binding. Thus the ligand and protein buffers must be carefully matched to ensure that the compositions of the buffers are identical. This may be achieved by dialyzing the ligand solution and the protein solution. Matching the buffer solutions may be difficult if the ligand, for example, is too small to be dialyzed. In this case, the protein may be dialyzed with an empty buffer solution and the ligand may be dissolved in the resulting dialysate. Another issue may arise if one of the molecules requires an organic solvent and the other an aqueous one. To accommodate this, if, for example, the ligand solution requires an organic buffer, the ligand and its buffer solution

should be diluted with the dialysate of the protein solution until the concentration of the organic buffer is below 1%. Because the ligand was already dissolved in the organic solvent, the serial dilution should prevent its precipitation. Additionally, a small amount of he organic solvent may be added to the protein solution in order to further decrease the organic solvent concentration mismatch.

Data

The raw output of the ITC experiment is power input to the reaction cell as a function of time as shown in Figure 2a. The area under each peak, i.e. the integral of the power data, corresponds to the heat produced by the binding reaction during that injection. When the quantity of heat generated by an injection is divided by the amount of ligand (in moles) contained in that injection and plotted against the ratio of the total amount of ligand and protein in the reaction cell the sigmoidal curve in Figure 2b is produced. Further, the amount of heat produced during an injection Q_i is,

$$Q_i = \Delta[ES]_i V_i \Delta H \, , \qquad (16)$$

where $\Delta[ES]_i$ is the change in bound enzyme concentration, V_i is the volume of the reaction cell and ΔH is the molar binding enthalpy.

Substituting the equilibrium values of the ligand and protein concentrations (equal to the total ligand and protein concentrations minus the bound enzyme concentration) into Equation 8 produces an equation relating the binding constant to the concentration of bound protein, the total protein concentration, and the total ligand concentration, [S_t],

$$K_b = \frac{[ES]}{([E_t]-[ES])([S_t]-[ES])} \, . \qquad (17)$$

The binding model in Equation 8 assumes that one protein binds with one ligand to form the product. In actuality a protein may have more than one binding site, each of which may interact with a ligand to produce a binding event. As such the actual binding

reaction can be modeled as the combination of one binding site and one ligand to produce a product, that is:

$$B + S \rightarrow P, \tag{18}$$

where B represents a binding site and P is the product of a single binding event. The analogous representation of the binding constant in Equation 17 is then,

$$K_b = \frac{[P]}{([B_t]-[P])([S_t]-[P])}. \tag{19}$$

If each protein has n binding sites then the concentration of binding sites $[B]$ is just the product of n and $[E]$. The binding product can still be arbitrarily represented by the letters "ES" allowing Equation 19 to be written as:

$$K_b = \frac{[ES]}{(n[E_t]-[ES])([S_t]-[ES])}. \tag{20}$$

Rearranging Equation 20 produces the following quadratic equation which specifies the equilibrium concentration of occupied binding sites after the ith injection.

$$[ES]_i^2 - \left(n[E_t]_i + [S_t]_i + \frac{1}{K_b}\right)[ES]_i + n[E_t]_i[S_t]_i = 0, \tag{21}$$

and the concentration of binding events that occur during the ith injection is:

$$\Delta[ES]_i = [ES]_i - [ES]_{i-1}. \tag{22}$$

Substituting this expression for $\Delta[ES]_i$ into Equation. 16 computes the amount of heat produced by each injection. A least squares optimization process is then used to compute the values of the binding parameters ΔH, K_b and n.
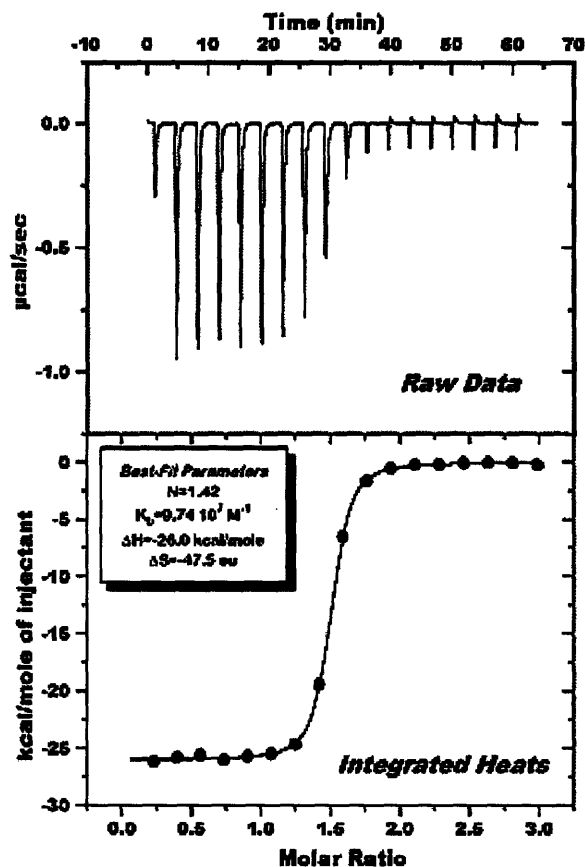
16

Figure 2: Power output and heat production per injection from an ITC experiment taken from MicroCal™ website

Binding Constant Range

In order to accurately determine the binding parameters of a reaction the system response to the ITC experiment, sigmoidal curve binding isotherm shown in Figure 2b, must have distinguishable features. Within the intermediate range of binding parameters the ITC response is unique and the binding parameters can be calculated with reasonable accuracy. However when the dimensionless parameter C defined as the product of the binding constant and the total protein concentration takes on extreme values, the utility of the ITC analysis is weakened.

Equation 8 gives the expression for the binding constant during a ligand-protein binding reaction. Rearranging this equation produces an expression for C,

$$C \equiv K_b [E]_t \approx \frac{[ES]}{[S]}. \tag{23}$$

When C is relatively low (less than 1), the concentration of bound protein is small and saturates almost immediately with the first ligand injection. Subsequent ligand injections do not bind to the protein and little useful ITC data can be retrieved. When C is relatively high (greater than 10,000) all the ligand that is injected in first several injections becomes bound to the protein. Once the ligand concentration reaches the value at which the binding reaction becomes saturated, no further binding occurs and no further heat is produced by the interaction. These two scenarios may occur in the case of extremely weak and extremely tight binding interactions, respectively. Figure 3 presents the binding isotherms for several orders of magnitude of C and how they lose their distinctiveness at extreme values of C.
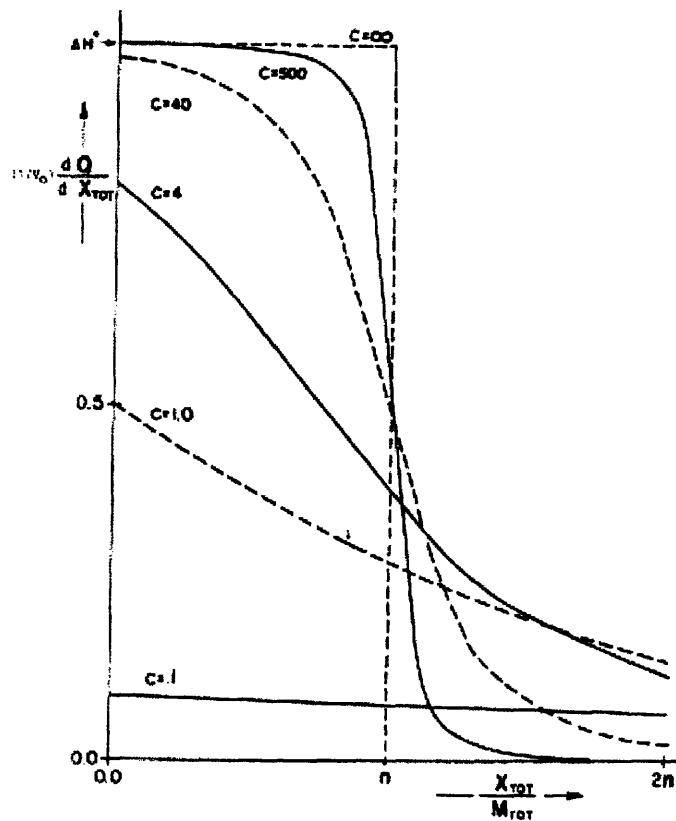

Figure 3: Binding isotherms for various values of C taken from Wiseman et. al.

The binding constant cannot be changed in the study of a given ligand-protein interaction. Therefore the protein concentration, $[E]_t$, provides a means of adjusting C. Large binding constants require small protein concentrations, and small binding constants require large ones. However, as the protein concentration decreases into the nano-molar

range the binding enthalpies become too small to be measured with current instrumentation

Macro-Calorimeter Experimental Design

In order to design and operate a precise and accurate nano-calorimeter, the process of isothermal titration calorimetry needed to be well understood without the complications of small reactant volumes and reaction enthalpies. To achieve this goal calorimetric titrations would be conducted on a so-called "macro" scale, with larger reactant volumes and larger reaction enthalpies. The primary objectives of the macro experiments were to detect heat via a change in temperature rather than a change in power consumption and, to use this data to calculate the binding constant and enthalpy of binding for a reaction while accounting for the similarly measured heats of dilution. Other objectives included preparing matched and buffered solutions and determining appropriate reactant concentrations.

Detecting heat through changes in temperature instead of changes in power consumption is a significant difference between the ITC procedure described above and the macro experiments. The isothermal property of the ITC process indicates that the temperature of the reactants must remain constant. This constraint allows reactions to be characterized at a single temperature and accounts for the temperature dependence of the binding constant, the molar binding enthalpy, and the reactants' heat capacities. The time-integral of the power consumption yields the amount of heat produced which is then used to calculate the reaction parameters. During the macro experiments, the reactants were not held at a constant temperature, rather, the change in temperature following an injection along with the heat capacity of the system were used to determine the amount of heat produced in the reaction.

Setup 1: Bench-top Calorimeter

The first attempt to collect calorimetric data consisted of beaker 1 which contained one of the reactants and beaker 2 which contained the second reactant. Both solutions were exposed to ambient and the temperatures of each were monitored. Ideally, both solutions would equilibrate to the ambient temperature and then a given volume of the second reactant would be injected into the first. Temperature measurements were made with resistance temperature detectors (RTD's) and data was digitally sampled. A magnetic stir bar was located in beaker 1 in order to allow sufficient mixing of the two reactants once they were combined. The entire setup was located in a fume hood in order to provide protection from any noxious gases.

The goal of the bench-top setup was to measure the dilution enthalpies for the mixing of methanol and dimethyl sulfoxide (DMSO) with water. The experiments conducted on the bench-top setup are summarized in Table 1.

#	Reactant 1	Reactant 1 Volume	Reactant 2	Reactant 2 Volume
1	100% Water	14 mL	100% Methanol	10 mL
2	100% Water	14 mL	2.5% Methanol	2.5 mL
3	2.8% DMSO	14 mL	3.0% DMSO	2.5 mL
4	2.5% DMSO	14 mL	3.0% DMSO	2.5 mL

Table 1: Summary of reactants and volumes used in bench-top calorimeter experiments.

Methanol and DMSO are both organic solvents into which ITC ligands might need to be dissolved. As stated above, in such cases, these organic solutions are then diluted with water to a low concentration, and the organic solvent is added to the enzyme solution in order to match the two buffers. Reaction 1 represented the case where a methanol based solution is not diluted before injecting it into the aqueous enzyme solution. This dilution reaction would produce large amounts of heat and thus serve as a proof-of-concept experiment for the bench-top calorimeter. Reaction 2 represented the case where the organic ligand solution was diluted but none of the organic solvent was added to the enzyme solution. Additionally, reaction 2 could be used to test the precision of the

20

system because it would produce much less heat than reaction 1. Reactions 3 and 4 were slight dilutions of DMSO that might occur if the DMSO/ligand solution was diluted, but too little DMSO was added to the enzyme solution.

The results from reactions 1-4 are shown in Figure 4. Several observations were made from this data including the effect of stirring, the time scale of the response, the accuracy of the system, and the importance of the temperature difference between the two reactants.
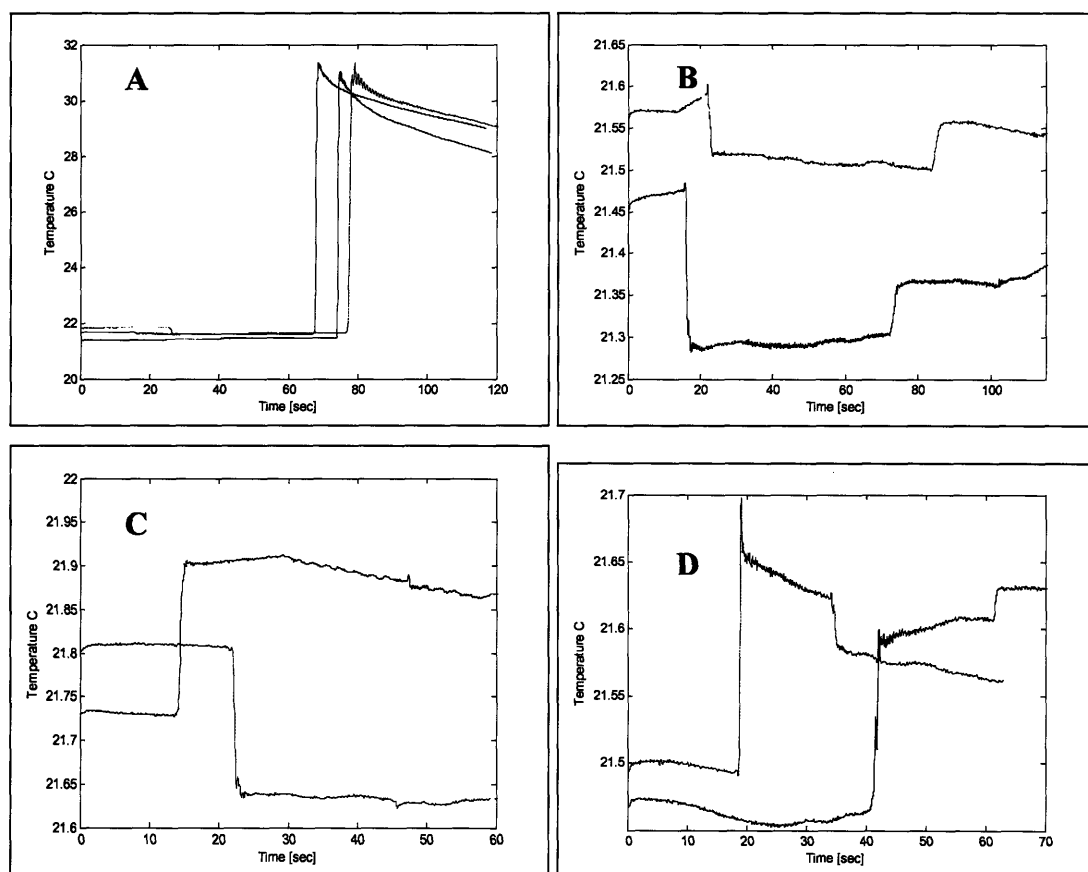

Figure 4: Temperature results from the dilution reaction conducted with the bench-top calorimeter. A is Experiment 1, B is Experiment 2, C is Experiment 3 and D is Experiment 4.

Effect of Stirring

In each experiment, before reactant 2 was injected into reactant 1, reactant 1 began to be stirred. The stirring manifested itself sometimes as an increase and sometimes as a

decrease in the temperature of reactant 1. Figure 5, however illustrates a control experiment where stirring was initiated in a volume of stationary water. The temperature immediately decreased and then slowly increased over the next 400 seconds. Two competing forces that would increase and decrease the water temperature are the work transfer from mixing and evaporative cooling, respectively. The motion of the stir bar does work on the water, increasing its internal energy and hence its temperature. On the other hand, as the internal energy of the water increases, so to does the kinetic energy of the water molecules. With increased kinetic energy, a greater proportion of molecules are able to exceed the energetic barrier to evaporate. Once these high energy molecules leave, the average kinetic energy of the remaining particles, and hence the temperature of the solution decrease. This mode of evaporative cooling however would occur on the same time scale as the heating due to the mixing. Experimentally, however the cooling occurs almost instantaneously which suggests an impulse rather than step change in the cooling rate.
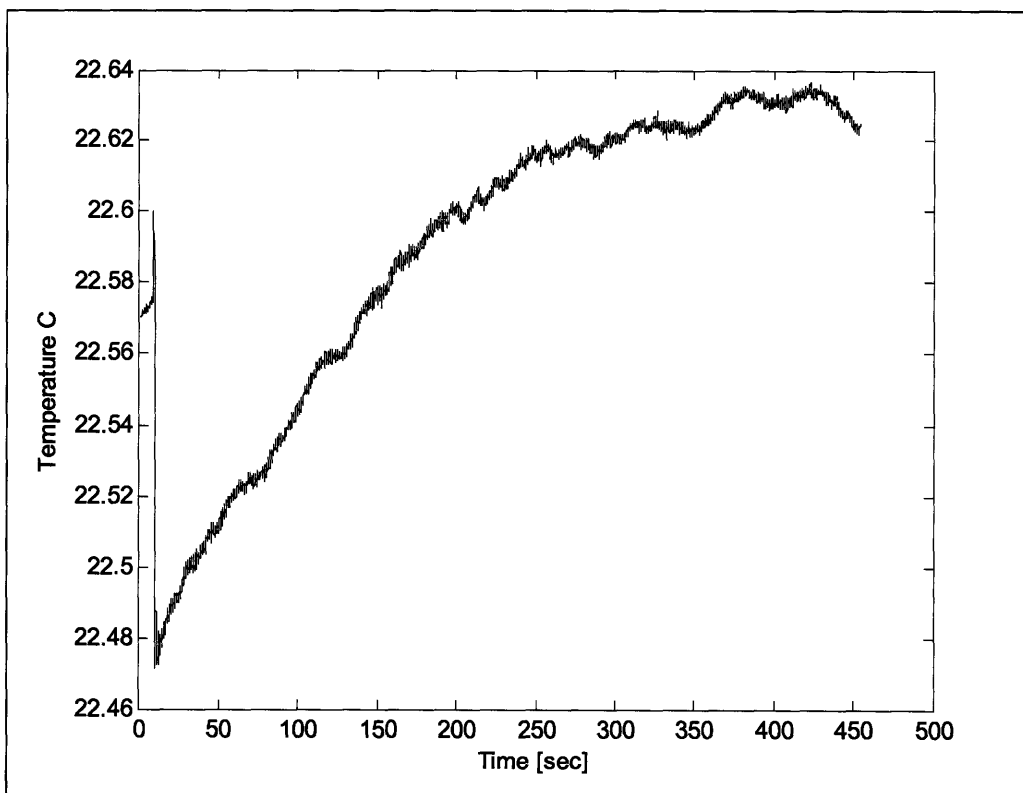

Figure 5: The temperature change caused by the initiation of stirring in a volume of water, the temperature drops almost instantaneously and then increases gradually.

The initial increase or decrease in the water temperature at the onset of stirring is most likely due to the elimination of thermal gradients in the fluid. These gradients are caused by 2 factors. First the temperature dependent density of the water causes the temperature of the water to decrease with increasing depth, and secondly, the unequal heating/cooling paths of the setup. For example, the heat transfer at the surface of the water would be less than that of the sides and bottom. Although these gradients exist in the water, the RTD only measures the local temperature of the water in contact with the sensor. When stirring begins, the solution very quickly becomes well-mixed, eliminating the temperature gradients and bringing the water to a single temperature. Depending on the location of the sensor and the nature of the temperature gradients, this new single temperature could be greater than, less than, or even equal to the initial pre-stirring temperature reading. Accordingly, at the onset of stirring an almost instantaneous increase or decrease in temperature is expected and exhibited in the temperature responses shown in Figure 4.

Time Scale

The temperature increase following the combination of the two reactants occurred over a time period on the order of one second. The relevance of this data depends on the rate at which the two reactants were combined. Because the injections were performed by hand, the injection speed varied and could not be measured accurately. Thus, with the onset of mixing, the generation of heat as well as its conduction throughout the fluid occurred at most over a time-scale of one second.

System Accuracy

Empirical data for the molar enthalpy of mixing water with methanol and DMSO is shown in Figure 6 along with a best fit curves based on the Redlich-Kister Equation (Equation 24), where ΔH^E is the molar enthalpy of mixing, x_1 is the mole fraction of one component of the mixture (in this case water), A_k's are adjustable parameters, and N is the number of adjustable parameters,

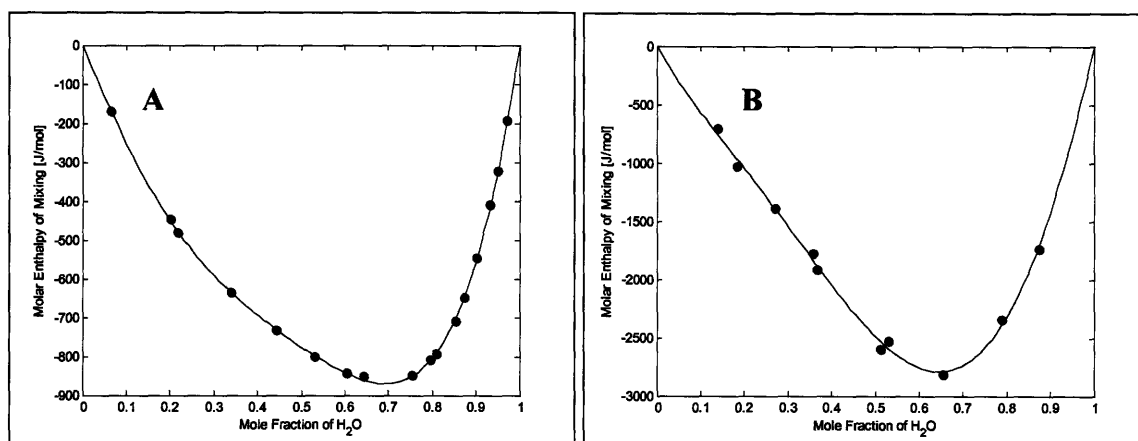$$\Delta H^E = x_1 (1 - x_1) \sum_{k=0}^{N-1} A_k (1 - 2x_1)^k .$$ (24)

Figure 6: Published values for the molar enthalpies of mixing Methanol (A) and DMSO (B) with water. The fit is based on the Redlich-Kister equation.

Using this data, expected values for the temperature changes associated with reactions 1-4 can be calculated. First the enthalpy of mixing for each reactant and product solution ΔH_i^E was calculated as shown in Equation 25 where N_{i1} and N_{i2} are the number of moles of pure substances 1 and 2 in solution i,

$$\Delta H_i^E = \left(N_{i1} + N_{i2}\right)\Delta H^E\left(x_{i1}\right). \tag{25}$$

The total amount of heat produced during the combination of reactants 1 and 2 is the difference between the enthalpy of mixing of the product and the sum of the enthalpies of mixing of the two reactants, Equation 26,

$$\Delta H_{1,2}^E = \Delta H_{product}^E - \left(\Delta H_{reac\tan t1}^E + \Delta H_{reac\tan t2}^E\right), \tag{26}$$

and the temperature change ΔT^E is given by Equation 27, where C_{total} is the combined heat capacity of reactants 1 and 2 and beaker 1,

$$\Delta T_{1,2}^E = \frac{\Delta H_{1,2}^E}{C_{total}}. \tag{27}$$

24

Table 2 lists the expected and measured temperature change for each reaction.

Reaction	Expected Temperature Change [°C]	Measured Temperature Change [°C]	% Error
100% Water/100% Methanol	9.00	9.56 ± 0.23	6.22
100% Water/2.5% Methanol	4.5×10^{-3}	$(5.9 \pm 0.21) \times 10^{-2}$	1200
2.8% DMSO/3.0% DMSO	0.118	-0.010 ± 0.002	-108
2.5% DMSO/3.0% DMSO	0.119	-0.008	-106

Table 2: Expected and measured results of bench-top calorimeter dilutions

Several factors contributed to the inaccuracy of the bench-top calorimeter dilutions. In some reactions the temperature change is almost zero or even negative. This is a result of the two reactants being at different temperature just prior to mixing. When this is the case, the temperature of the final solution changes to the heat capacity weighted average of the two reactant temperatures and then rises due to the enthalpy of mixing. If the temperature of reactant 2 is sufficiently different than that of reactant 1, the temperature change due to the dilution is completely masked by the temperature equilibration. Although attempts were made to allow the two reactants to equilibrate to identical temperature, it is possible that thermal gradients and different heat conduction pathways existed in the ambient setup that allowed the reactants to settle to different temperature. Moreover, this fact is confounded by the lack of precision in the RTD sensors which may differ by more than 300 mK.

The stirring of the solutions both altered the temperature of reactant 1 prior to the injection and added noise to the system. While the noise could be filtered out as shown in Figure 7, the temperature change contributed to the temperature mismatch described above.
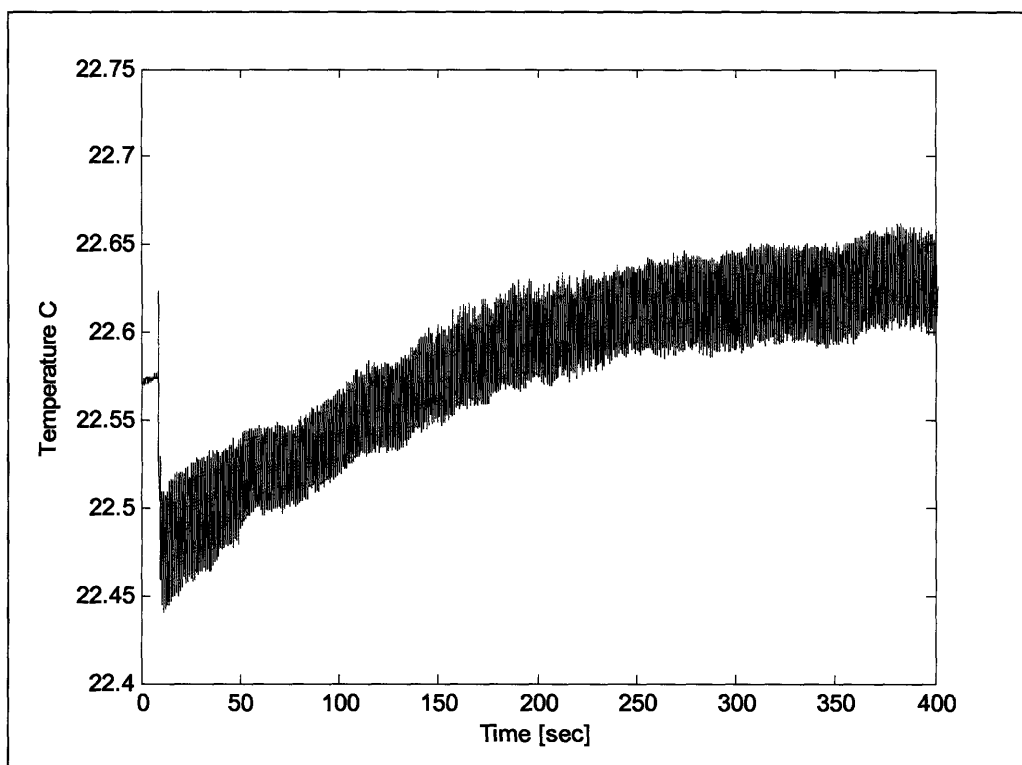
Figure 7: The temperature response to the initiation of stirring water. This is the unfiltered version of the response in Figure 5.

Additional sources of error included the precision of each injection and the inability to control the thermal character surrounding the environment. Also, the data used as a basis for the expected results relates to reactions that occur at 25 °C, whereas these reactions were conducted at ~21.5 °C. The enthalpy of mixing is temperature dependent and increases with temperature, thus, the measured values should be less than the expected ones.

Because the temperature rise time was much smaller than the time constant of the heat loss, the change in temperature could be calculated as the difference between the solution temperature just prior and just after the injection.

Setup 2: Isoperibol Macro-Calorimeter

In order to address the issues inherent in the design of the bench-top calorimeter described above, an isoperibol calorimeter was designed. An isoperibol calorimeter varies from an isothermal calorimeter in that the temperature of the system is allowed to change, and it is this temperature change that is used to detect the heat production. This is the same principle employed by the bench-top calorimeter. In an isoperibol calorimeter it is important that the greatest possible proportion of heat produced is sensed as a temperature change, thus there must be a minimal heat transfer between the system and its environment. An isoperibol calorimeter is not to be confused with an adiabatic calorimeter which operates on the principle that there is zero heat transfer between the calorimeter system and the environment. In an adiabatic calorimeter the reaction chamber is encased by a thermally controlled jacket whose temperature changes precisely with that of the reaction chamber in order to prevent any heat transfer between the two. An isoperibol calorimeter differs from an adiabatic calorimeter in that there is no heat compensation; rather the system is designed with a small but finite heat transfer that can be modeled and incorporated into the data analysis.

The goal of the isoperibol calorimeter was to allow the two reactants to equilibrate to an identical temperature and to minimize and model the heat pathways out of the system. A schematic of the isoperibol calorimeter is shown in Figure 8. The reaction chamber is a glass vial mounted atop a block polystyrene insulation in the center of a large brass enclosure. The entire brass block is suspended in a temperature controlled water bath. An air gap between the glass vial and the brass enclosure decreases the heat transfer between the two and simulates an adiabatic vacuum chamber. The large thermal masses of the brass block and the water bath allow the brass/water couple to serve as a constant temperature heat sink. The brass will slowly change temperature and any temperature gradient between the brass and the water bath will be absorbed by the even larger thermal mass of the water and the temperature of the two will remain relatively constant.
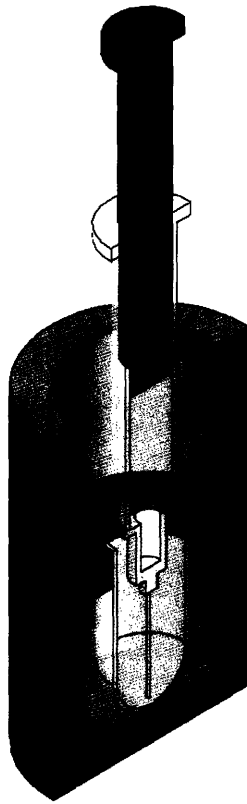
Figure 8: A model of the isoperibol calorimeter. The reaction vial is situated inside a brass block which is placed inside a 1.3 L water bath (not shown). The syringe was connected to two motors: one to control injections by moving the plunger and the other to raise and lower the syringe as a whole.

The isoperibol calorimeter system can be modeled as an arrangement of electrical components as shown in Figure 9. Resistors represent the various thermal resistances; capacitors represent the heat capacity of each component, and the current source represents a thermal power input. The thermal elements of the water bath, save its constant temperature, have been excluded from the model since its thermal mass is almost an order of magnitude greater than that of the brass block. Based on this model, the system response due to a power impulse of 1.0 W is shown in Figure 10. As expected the temperature of the brass block remains constant confirming that the temperature of the water bath will do the same.
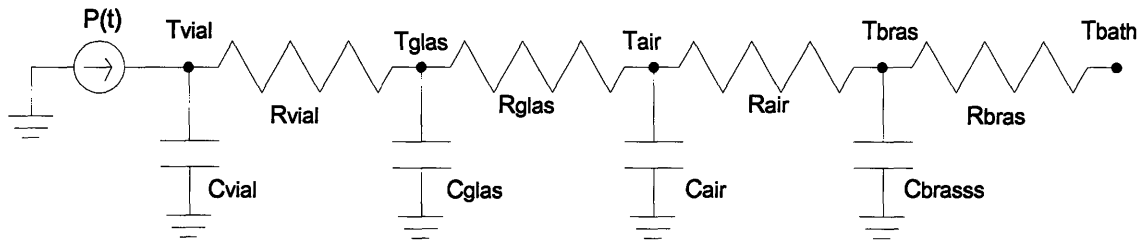
Figure 9: Lumped thermal capacitance model of the isoperibol calorimeter. Resistors represent thermal resistances, capacitors represent heat capacities, and the current source represents a power input.
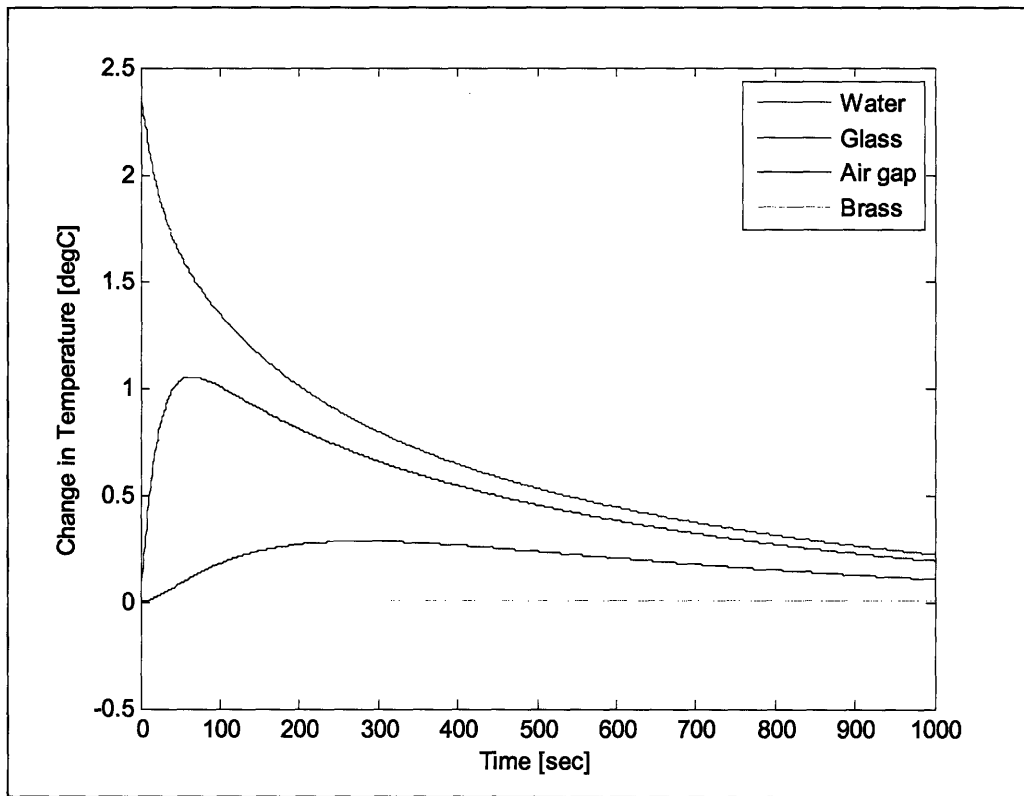

Figure 10: Theoretical model of the isoperibol calorimeter response to an impulse of 1.0 W into the system at *t=0*.

The temperatures of the water inside the glass vial and the glass vial itself are in thermal contact, but the temperature of the water is able to increase significantly before dissipating heat to the glass and closing the temperature gap between the two. All of the heat is instantaneously absorbed by the water and its temperature immediately spikes as if there were no other thermal masses in the system. This is because the model assumes that the heat is delivered instantaneously and that the water is capable of heating in its entirety in a single moment. Figure 11 illustrates the case when a constant power input of

0.1 W is delivered over the course of 10 seconds, effectively delivering the same amount as the power impulse but at a slower rate. The temperature of the water no longer increases with infinite velocity, but the model still assumes that the water warms as a whole and there is no time lag between the onset of heating and the onset of temperature change.
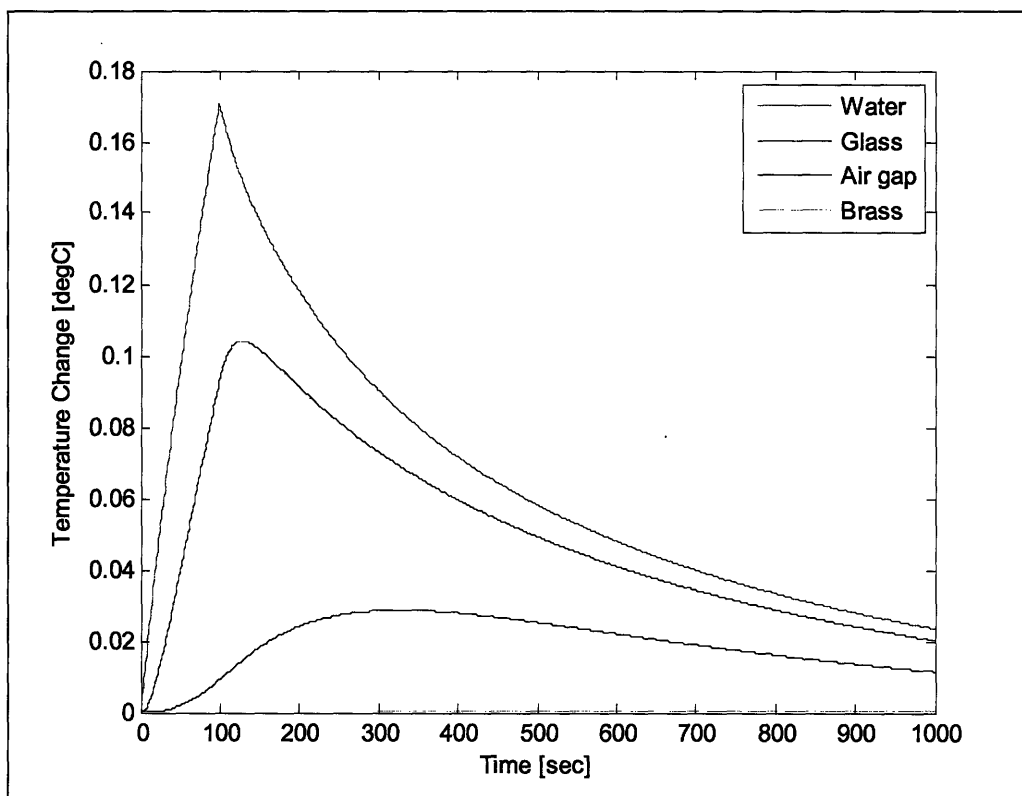

Figure 11: Theoretical model of the isoperibol calorimeter response to a 100 second input of 0.01 W into the system at starting at *t=0*.

In practice, in order to achieve a uniform and near instantaneous change in temperature resulting from a chemical reaction it is necessary that the reacting solution be well mixed. Mixing the solutions via shaft work changes the dominant mode of heat transfer from natural to forced convection. The bulk motion of the fluid not only serves to conduct heat more quickly through the water, but also to mix the reacting species and allow the reaction to not be rate limited by mass diffusion. Figure 12 illustrates the effect of mixing the contents in the vial while inserting a 10 second pulse at 0.1 W. Because the model already assumes the water heats uniformly, no increase in lag time between heating and temperature change is apparent. However, the conversion to forced

convection heat transfer has decreased the thermal resistance of the water and more closely coupled the water to the vial. This offers the advantage of placing RTD's outside of the vial so as to not interfere with the reaction or serve as a heat path from the water to ambient.
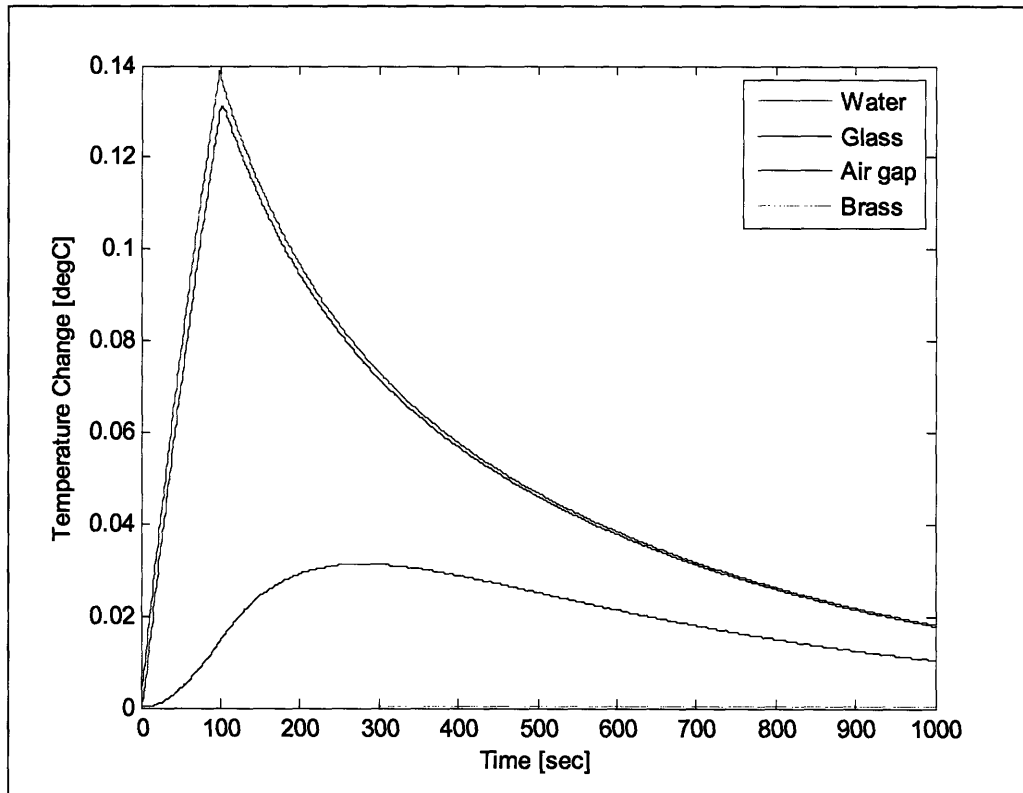

Figure 12: Theoretical model of the isoperibol calorimeter response to a 100 second input of 0.01 W into the system at starting at *t=0* with mixing.

Experimental Thermal Characterization

In order to test the isoperibol calorimeter thermal model, controlled amounts of heat were added to 1 mL of water inside the reaction vial. In the first set of simulations a surface mount resistor was placed inside the water and used as a resistive heating element in the absence of mixing. Figure 13 summarizes the results of these experiments. The most noticeable difference between this data and the theoretical model is the absence of an immediate increase in temperature followed by a sharp decrease. Rather, there exists a lag between the onset of heating and the temperature increase as well as a gradual decrease in the heating rate as the water dissipates heat to its surroundings. This transient is primarily due to the effective point source nature of the heating element. The system

31

requires time to spread heat throughout the glass and water. Because the heating occurs more slowly, there is also more time for heat to be dissipated to the surroundings. Indeed there exist heat paths out of the system that were not included in the thermal model: most notably to through the unsealed top of the brass enclosure and the RTD sensors in contact with the vial and solution.
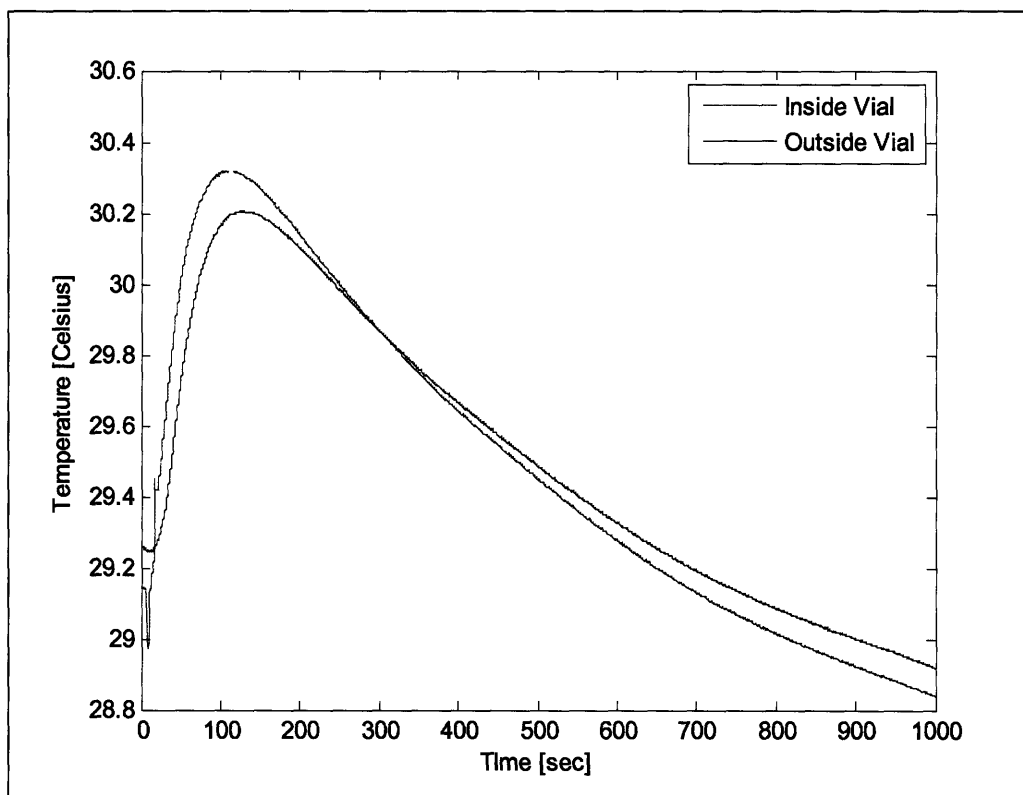

Figure 13: Measured temperature response of the isoperibol calorimeter when 1 W is delivered for 8.3 seconds through a surface mount resistor.

To increase the rate of bulk heating, a more volumetric heating element was chosen. A coil of Ni-Cr wire was placed inside the reaction vial, and a current was passed through it. In this manner, rather than heating the water from a single location, heat was produced along the entire length of the submerged wire. The results of this experiment are shown in Figure 14. Although this response resembles the idealized model more so than the case of the surface mount resistor, a distinct peak temperature is never achieved as the rate of temperature change decreases and then becomes negative. Although the heating is

32

spread more uniformly in the fluid, the heat transfer rate continues to be slowed by the dissipation out of the system.
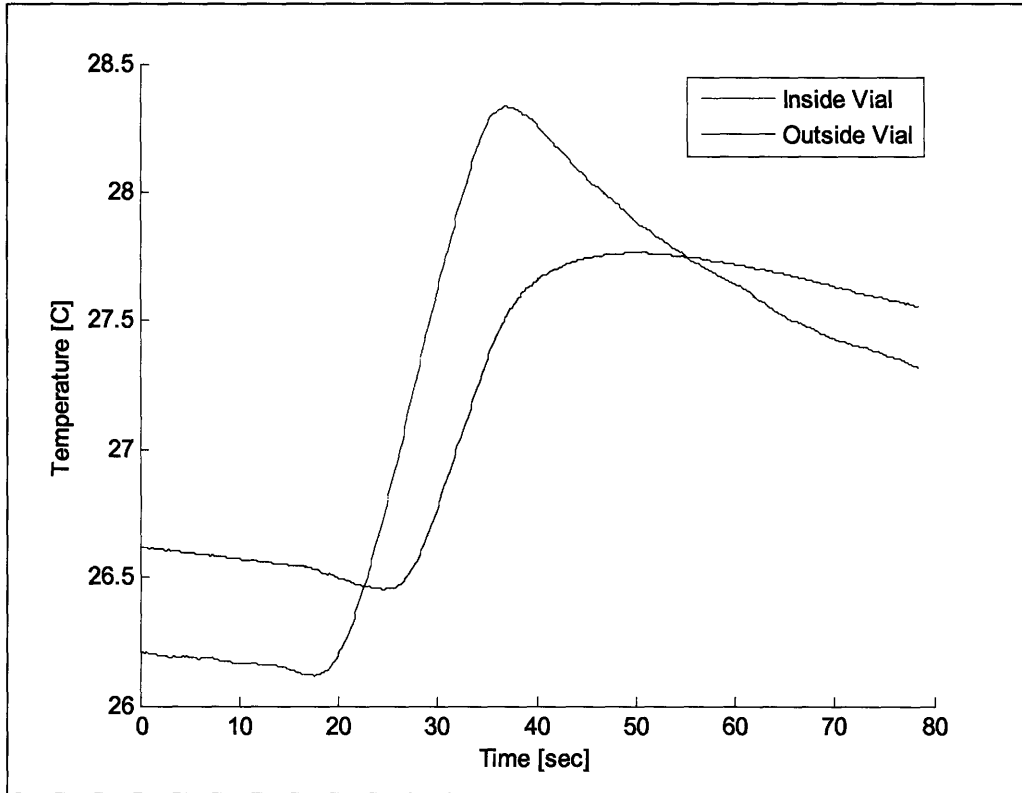

Figure 14: The temperature response of the inside and outside of the glass vial when 0.645W was delivered for 15 seconds through a coil of Ni-Cr wire.

To increase the rate of heat transfer within the water a magnetic stir bar was used to mix the solution while heat was added. Figure 15 depicts the result of this process. Here the temperature increases linearly with the heat input and nearly peaks as the heating concludes. This result confirms the behavior seen in the response of the theoretical model to a constant power input.
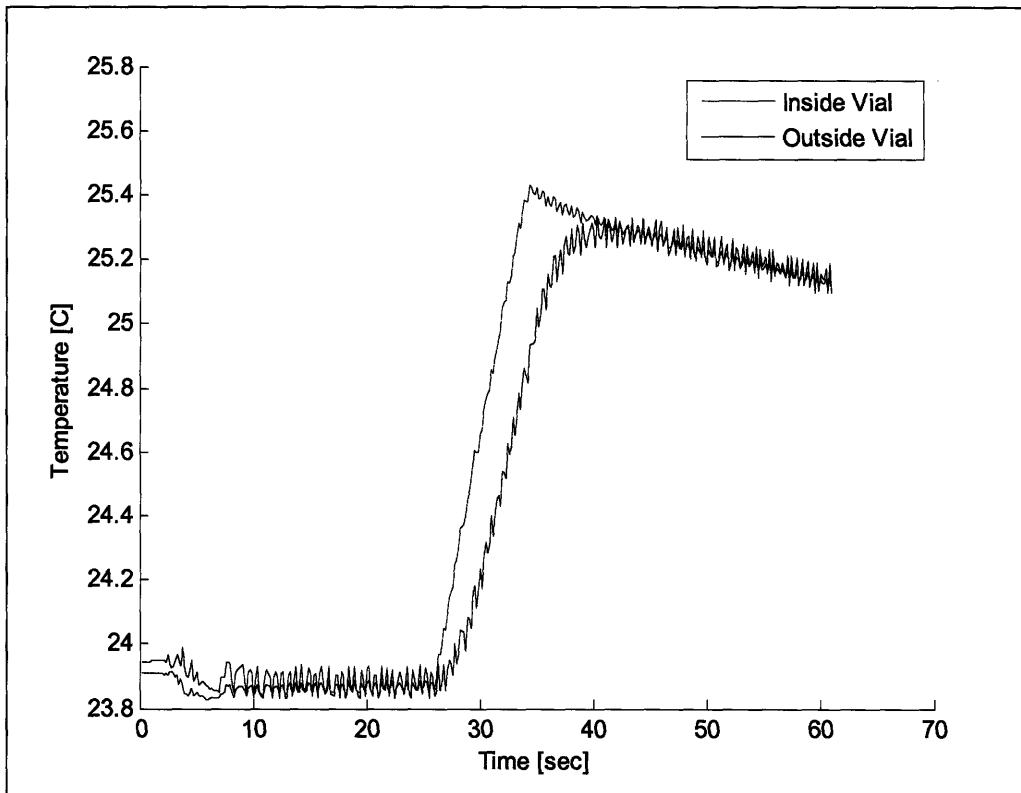
Figure 15: The temperature response of the inside and outside of the glass vial when a magnetic stir bar is used to rapidly distribute the heat input throughout the liquid.

In order to investigate whether the impulse response of the theoretical model was an accurate limit of the isoperibol calorimeter, it was necessary that the system be subject to an input that would cause an instantaneous change in temperature. One option would be to input a very short current pulse into a resistive heating element in the water, but this would require a large current source not readily available from an Agilent 33220A Function Generator. Another option would be to cause an instantaneous change in the heat transfer rate into the water. This was achieved by allowing the water to be at a cooler temperature than its surrounding and eliminating thermal gradients in the water via calm mixing. At this point the temperature of the water was increasing slowly to come to equilibrium with the water bath and other components. During this time, the stir bar was used to initiate vigorous mixing which increased the coefficient of convection for the water, an effective step input into the system. The convection coefficient can range over several orders of magnitude depending on the motion of the fluid, thus mixing the fluid

can result in large change in the rate of heat transfer. As shown in Figure 16, the temperature of the water increased very rapidly as a quantity of heat was drawn in from the surrounding bodies. This is confirmed by the decrease in the temperature of the outer surface of the glass vial at the onset of mixing and the gradual increase in its temperature after the mixing was terminated and the over-heated water began to lose heat back to its surroundings.
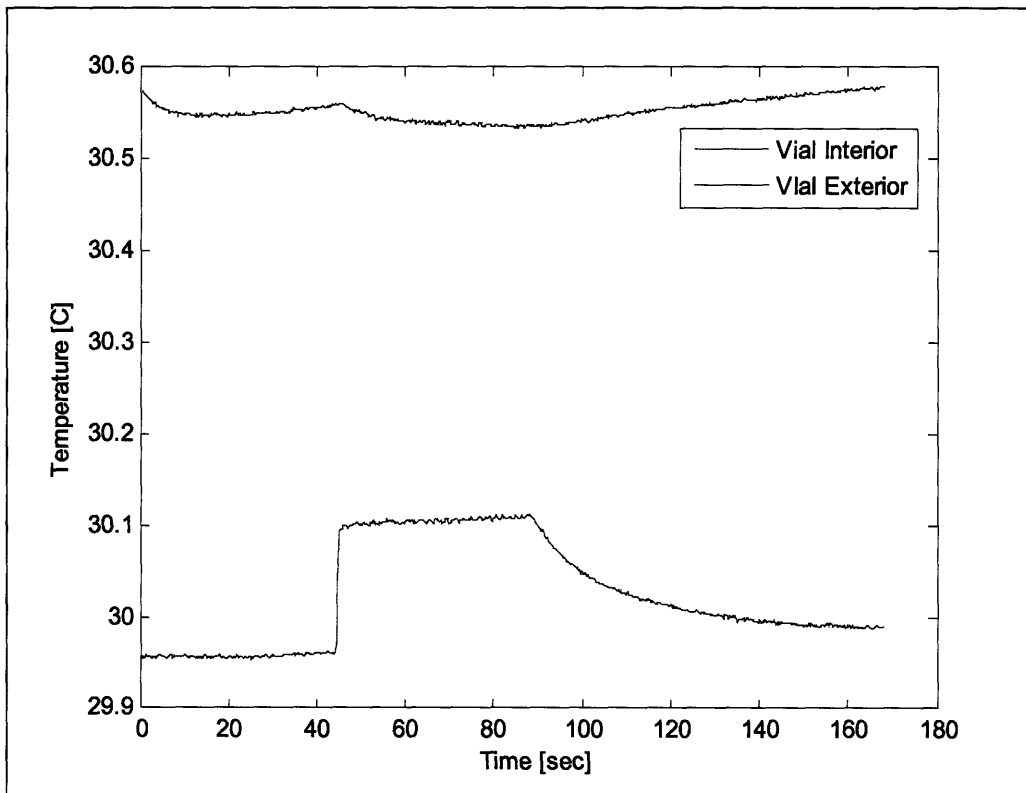

Figure 16: Very rapid temperature increase in the vial at the onset of mixing. This is likely due to a large heat transfer from the warmer environment due to the increase in the convective heat transfer coefficient.

In sum, the difference between the responses of the theoretical model and the experimental model stem from the idealized inputs to the theoretical system. In practice impulse and step power inputs are difficult to produce. In reality inputs increase and decrease over finite periods of time as shown in Figure 17. These differences account for the lack of sharp peaks in the experimental data.
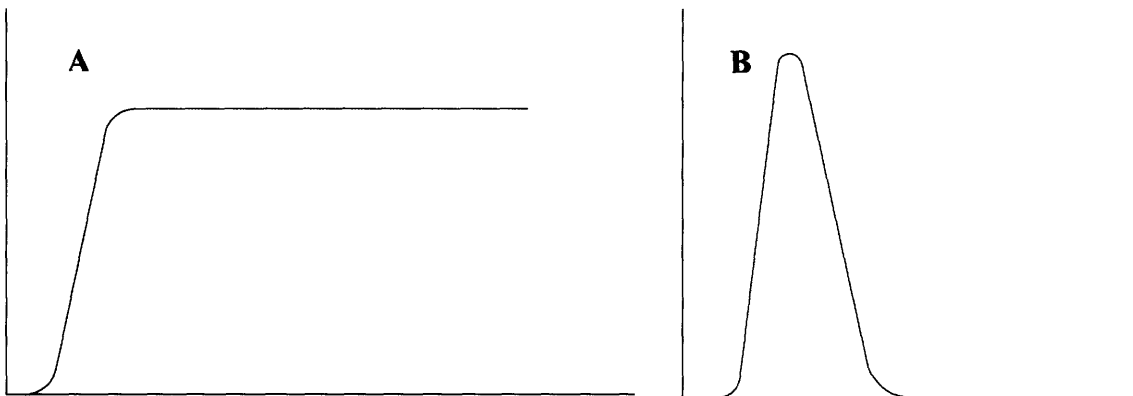
Figure 17: A) The practical continuous representation of a step function. B) The practical continuous representation of an impulse function. Both signals lack sharp cusps or vertical regions indicative of instantaneous change.

The resolution of the isoperibol calorimeter is another important system characteristic. While the RTD output is provided to a sensitivity of 1 mK, the noise level is between 5 and 6 mK. Thus any temperature change below that level would not be discernible.

With the knowledge that the experimental system will not peak to its maximum temperature i.e. that some of the heat generated by a reaction will be dissipated before it causes an increase in the water temperature, a method must be developed to determine the peak temperature or the total amount of heat generation. In order to determine the amount of heat that was produced by a reaction, deconvolution can be employed to yield the power input to the thermal system. The theoretical isoperibol model is a solution two a set of 4 linear, constant-coefficient differential equations and is a linear time-invariant system. For a given chemical reaction the experimental temperature data is the output to the thermal power that went into the system due to the chemical reaction. To determine this unknown input, the data processing must utilize the system response and the system characteristics to work backwards to a unique solution. To do this, a simpler model of the system is useful. Figure 18 illustrates the temperature drop of the theoretical model after an initial increase. This response is will fit with a first order exponential decay. Thus a simple RC circuit can be used to produce this exponential response.

For a system with transfer function $H(s)$, the input $x(t)$ and output $y(t)$ are related in the Laplace domain by Equation 28,

$$Y(s) = X(s)H(s). \tag{28}$$

If the system input takes the form of a unit impulse function, $\delta(t)$, then $X(s)$ equals one the output of the system in the Laplace domain is,

$$Y(s) = H(s). \tag{29}$$

Performing the inverse Laplace transform yields the response to the unit impulse in the time domain.

Deconvolution is premised on the principle illustrated in Figure 19 - that the arbitrary input signal $x(t)$ can be represented as the sum of an infinite series of scaled and shifted unit impulse function, that is, with infinitely small spacing,

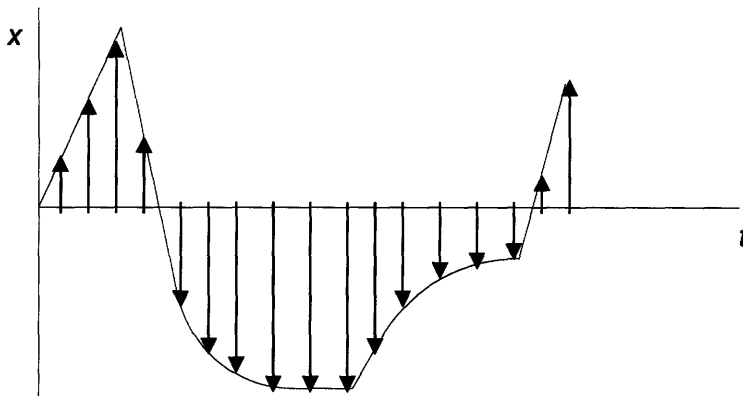$$x(t) = \int_{-\infty}^{\infty} x(\tau)\delta(t-\tau)d\tau. \tag{30}$$

Figure 19: An arbitrary signal $x(t)$ is shown as a series of shifted impulse functions which may be scaled by the value of x at that point and the spacing between the pulses.

It follows from the linearity of the system that if an input $x(t)$ is the sum of scaled and shifted unit impulse function inputs then its output, $y(t)$, is the sum of the outputs to these scaled and shifted unit impulses. Since $h(t)$ is the output of the unit impulse input located

37

at $t=0$, then $h(t-\tau)$ is the output to the shifted unit impulse $\delta(t-\tau)$. Thus the output given by the input $x(t)$ is,

$$y(t) = \int_{-\infty}^{\infty} x(\tau)h(t-\tau)d\tau, \tag{31}$$

and $y(t)$ is the convolution of $x(t)$ and $h(t)$.

For the isoperibol calorimeter the temperature output is $y(t)$ and the unknown power input is $x(t)$. The unit impulse response is the time domain equivalent of $H(s)$ given by,

$$H(s) = \frac{R}{RCs+1}. \tag{32}$$

The discrete deconvolution of temperature output and unit impulse response yields a discrete data set $x(t)$ which is integrated from the beginning to the end of one reaction to determine the heat produced therein.

Isoperibol Calorimeter Results

DMSO Enthalpy of Mixing

To test the ability of the isoperibol calorimeter to produce accurate and repeatable data during heat of dilution control reactions, a series of dilutions were conducted with the DMSO and water. During the first set of dilutions the reaction vial initially contained 1.4 mL of 100% DMSO, and the syringe contained 0.5 mL of 100% deionized water. The contents of the vial and syringe were allowed to equilibrate to within 30 mK of each other, and then 0.25 mL of water was injected into the DMSO. Approximately 640 seconds later a second injection 0.25 mL was made into the reaction vial. This process was repeated 4 times. The results of the DMSO dilutions are summarized in Table 3 and compared with the literature values presented above.

Injection	Expected Heat Output [J]	Measured Heat Output [J]	%Error
1st 0.25 mL injection	70.86	52.64 ± 4.76	-25.71
2nd 0.25 mL injection	58.96	36.64 ± 2.22	-38.1

Table 3: Comparison between expected and measured DMSO heats of dilutions.

Whereas with the bench-top calorimeter dilutions the expected heat output was divided by the thermal mass of the system in order to yield the expected temperature change, in the analysis of the isoperibol calorimeter dilutions, deconvolving the temperature data, Figure 20a, determined the power inputs, Figure 20b, to the system which was then integrated to calculate the heat outputs above. The excess molar enthalpies for the dilutions of the water into DMSO/water mixtures were calculated assuming the initial reaction had occurred as expected based on the Redlich-Kister model.
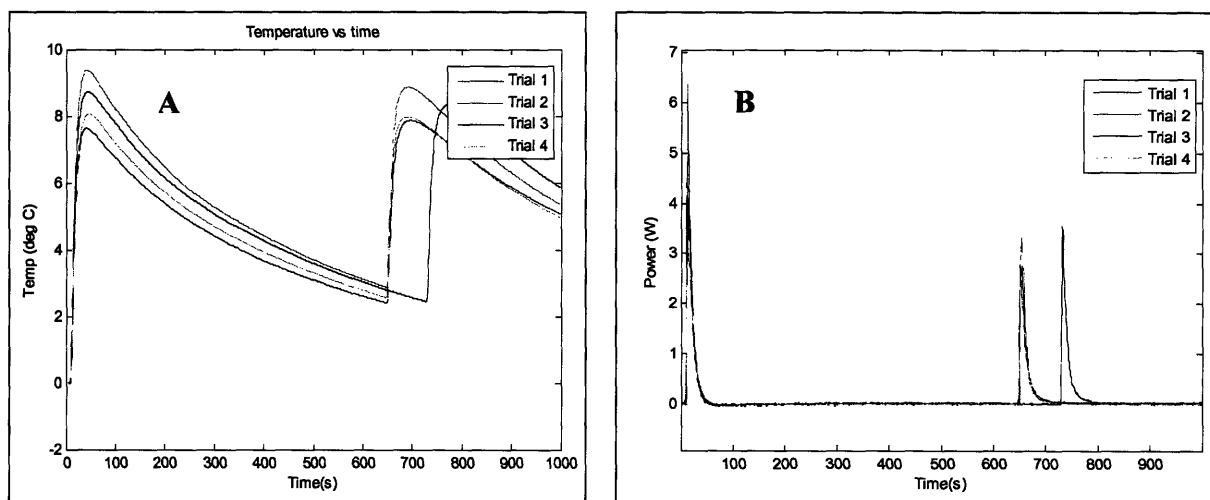

Figure 20: A) The changes in temperature associated with the injection of water into the DMSO solution. B) The deconvolved power input that models the rate of heat transfer into the system.

Analysis of MicroCal™ ITC Data

A complete set of data for the titration of Acetazolamide into Carbonic Anhydrase II was provided by Pfizer. The raw data is shown in Figure 21a. In order to better understand the ITC process, this data was used to recreate the analysis performed by the MicroCal™ software Origin. First the data was filtered in order to remove the baseline drift of the measurements, see Figure 21b. Then the data was integrated from the beginning of each injection until the following injection in order to produce the heat generated by each injection, see Figure 21c. In this particular analysis the control dilution experiments had not been performed. Instead the heats generated by the final 8 injections were averaged and subtracted from each heat of injection. The least-squares fit for the following model was then used to determine the binding constant K, the stoichiometric ratio n, and the enthalpy of binding ΔH.
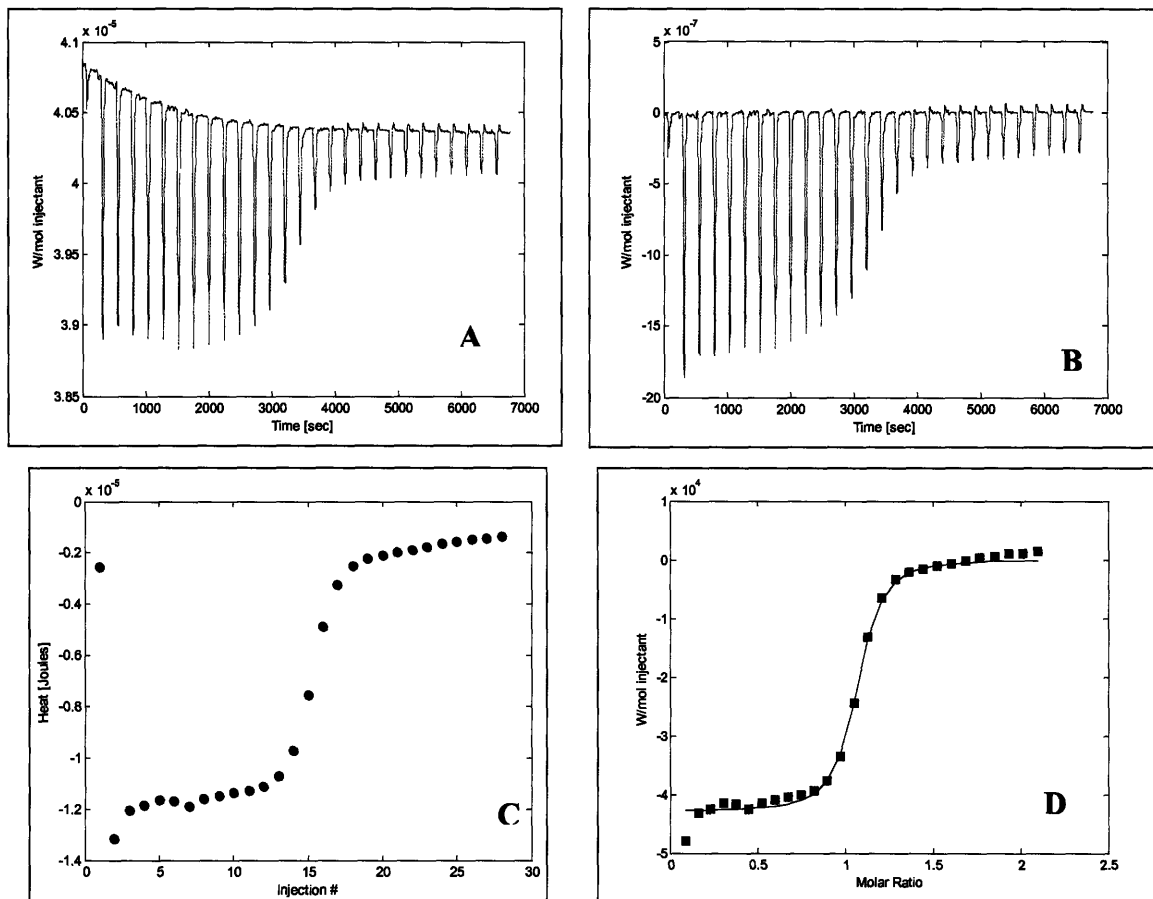
Figure 21: A) The raw ITC power data. B) The raw ITC power data with the baseline drift removed. C) The heat generated with each injection. D) The binding isotherm for the interaction

The binding isotherm for the derived fit along with the results of the Origin software are plotted in Figure 21d. Table 4 contains the binding parameters for this data. As shown in the comparison between the percent error between the derived values and the Origin values and the percent uncertainty reported with the Origin data, the above analytical procedure was able to accurately reproduce the Origin algorithm.

Parameter	Derived Values	Origin Values	Error [% Origin Value]	Origin Uncertainty
K [M^{-1}]	2.152×10^7	2.17×10^7	-0.829	13.2%
n	1.037	1.04	-0.288	0.486%
ΔH [J/mol]	-1.027×10^4	-1.030×10^4	-0.291	0.801%

Table 4: Comparison of Origin ITC parameters - binding constant, stoichiometric ratio, and enthalpy of mixing - to those calculated in this study. All the calculated values are within the uncertainty boundary of the Origin calculations.

Acid-Base Titrations

The neutralization reaction between an acid and a base was employed to create data from which the binding parameters K and ΔH could be derived. These reactions produce moderate amounts of heat and the diversity and cost of reactants makes the neutralization reaction easily scaled up to high concentrations that can produce temperature changes well above the noise floor of the isoperibol instrument. The chosen reactants were hydrochloric acid, HCl, and ammonium hydroxide, NH$_4$OH. The overall reaction is summarized by,

$$HCl + NH_4OH \rightarrow H_2O + NH_4Cl . \tag{33}$$

To find the molar enthalpy of the reaction, the molar enthalpies of formation of the reactants were subtracted from the molar enthalpies of the products yielding a value for $\Delta H_N = -52.22$ kJ/mol. The acid dissociation constant, $K_A = 10^8$ for HCl is the equilibrium constant for the production of hydrogen cations and chlorine ions. Similarly, the base dissociation constant, K_B, for NH$_4$OH is the equilibrium constant for the production of hydroxide and ammonium ion concentrations in solution.

The equilibrium constant, $K_N = 1.778 \times 10^2$ M^{-2}, for the overall reaction is the product of the acid and base dissociation constants.

42

Two types of titrations were conducted: 0.050 mL injections of 1.33 M NH₄OH into 1.0 mL of 1.0 M HCl and 0.050 mL injections of 1.33 M NH₄OH into 0.75 mL of 1.0 M HCl. The results of one such titration are shown in Table 5 and Figure 22.

Parameter	Measured Values	Theoretical Values
K_N [M^{-2}]	1.109×10^3	1.778×10^3
ΔH_N [J/mol]	-2.67×10^4	-5.222×10^4

Table 5: Comparison of measured and theoretical reaction parameters for the neutralization reaction between HCl and NH₄OH.
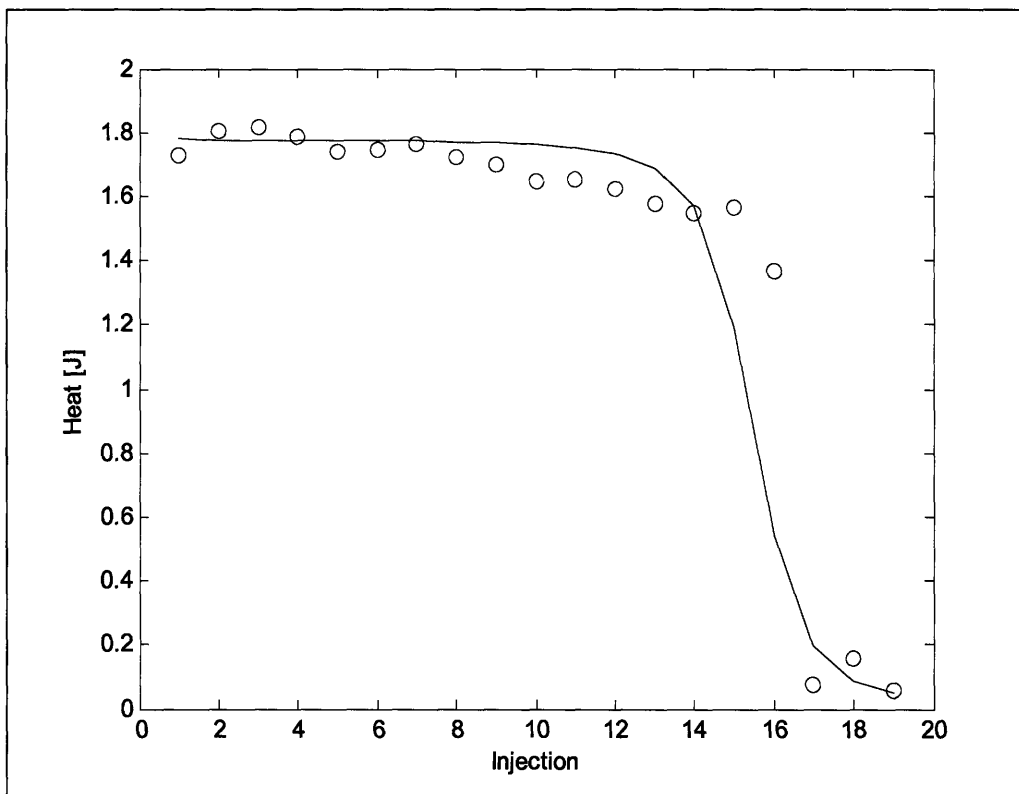

Figure 22: The amount of heat produced by each acid-base injection. The points are the experimental data and the curve is fitted model.

The difference between the fitted and theoretical equilibrium constants is likely due to the imprecision in measuring the very high acid dissociation constant of HCl. The difference in enthalpy of neutralization is likely due to the very rough calibration of the isoperibol

calorimeter which stemmed from the difficulty in injecting a well characterized volumetric heating.

Enzyme Kinetics Model

The concept of the relative binding tendency of a ligand to an enzyme was introduced previously. On the basis of the strength of binding, an association may be characterized as tight or weak; while on the basis of the rate at which this binding occurs an association may be either fast or slow. In order to see the effect of the binding strength and speed on the result of an enzyme-ligand interaction, a model was developed to describe the transient response to the binding reaction between an enzyme and ligand. Using Equations 7 and 9, the first-order non-linear differential equation,

$$\frac{d[ES]}{dt} - k_f[ES]^2 + k_f\left([E_t]+[S_t]+\frac{1}{K_b}\right)[ES] = k_f[E_t][S_t], \qquad (34)$$

was derived to model the creation of the enzyme-substrate complex. Given the total amounts of enzyme and ligand in a system, the solution to Equation 34 yields the concentration of bound enzyme as a function of time.
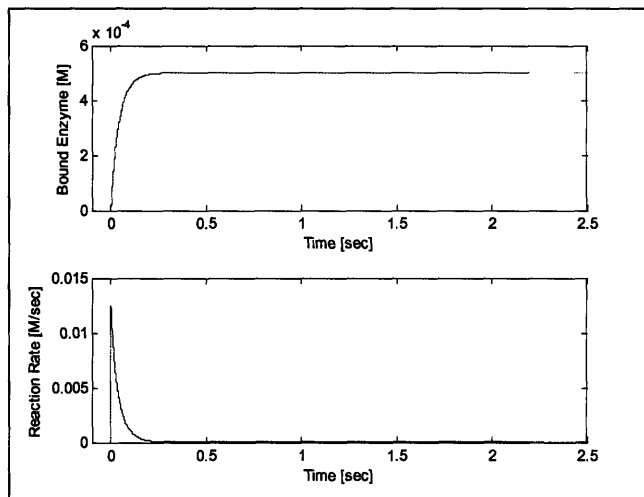
The strength and speed of a binding reaction are determined by the binding constant and forward rate constant included in Equation 34. Reasonable values of these constants that would yield the different combinations of tight or weak and fast or strong characteristics are shown in Table 6.

|	**Tight**	**Weak**
Fast	$K_b = 1\times10^{10}$ $k_f = 1\times10^4$	$K_b = 1\times10^{-2}$ $k_f = 1.5\times10^{-1}$
Slow	$K_b = 1\times10^{10}$ $k_f = 5\times10^{-1}$	$K_b = 1\times10^{-2}$ $k_f = 1\times10^{-5}$

Table 6: Generic values of the binding constant K_b and the forward rate constant k_f that yield the various combinations of a tight and fast, tight and slow, weak and fast, and weak and slow binding reaction. The units for K_b and k_f are M^{-1} and $M^{-1}\ sec^{-1}$ respectively.

The enzyme production and rate of enzyme production for each of the systems listed in Table 5 are shown in Figure 23. Note that in tight binding systems, all of the 0.5 mM of initially free enzyme is converted to bound enzyme. The reaction proceeds to completion because the large binding constant pushes equilibrium toward the creation of the enzyme substrate product. The difference between the fast and slow reactions is apparent as the slow reactions take nearly 5000 seconds to reach equilibrium while the fast reactions are completed in less than 0.5 seconds. The binding constants for the two tight reactions are equivalent as are the binding constants for the two weak reactions. However, the forward rate constants differ for all four reactions. This is because the reverse rate constant is the ratio of the forward rate constant and the binding constant. In order for a reaction to be considered slow, both rate constants must be relatively small. However, for a reaction to be fast, the rate constant in the dominant direction of the reaction must be large while the other is small. In the tight fast reaction, the dominant direction is forward and the reverse rate constant is only 10^{-6} sec^{-1}. Alternatively, in the weak fast reaction, the reverse reaction is favored, and so the reverse rate constant (15 sec^{-1}) exceeds k_f.
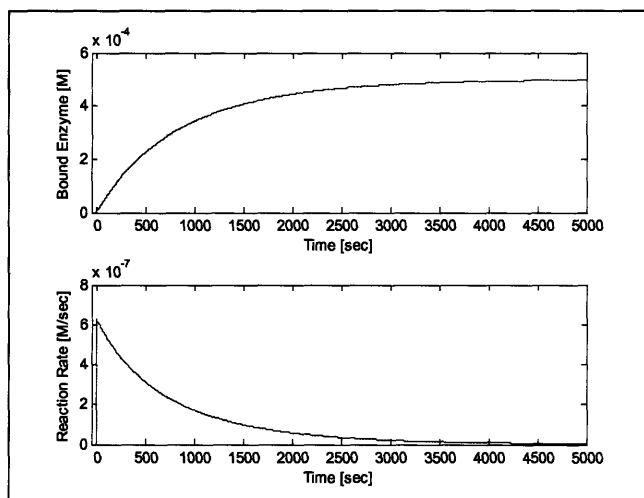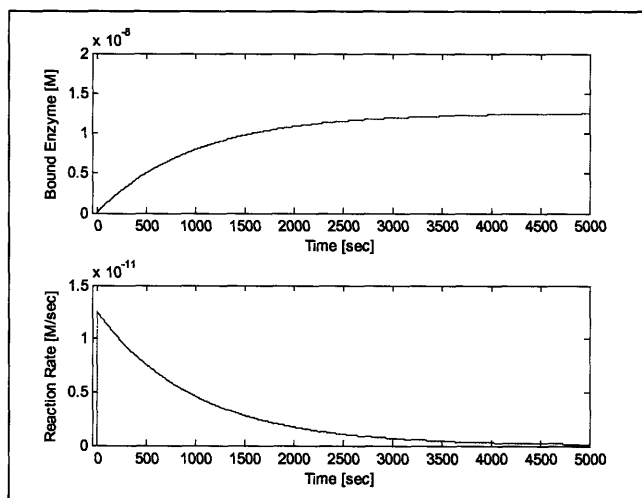
45
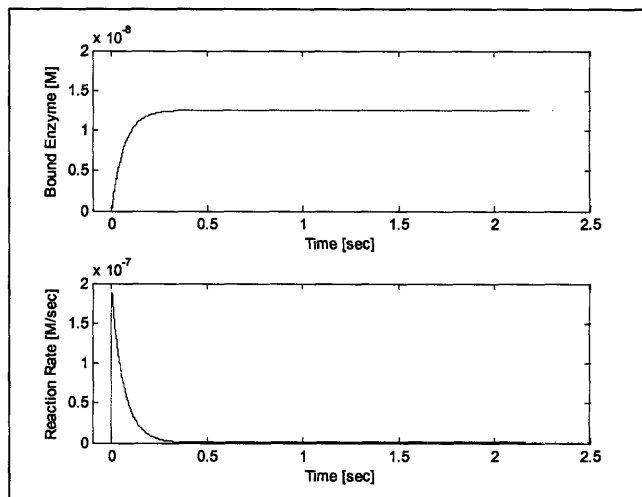
Figure 23: Models of tight, slow, fast, and weak enzyme binding reactions. Each reaction includes a 0.5 mM enzyme solution and a 2.25 mM ligand solution. The binding constants and forward rate constants for each reaction are given in Table #. Note that the time scale for the slow reactions is 3 orders of magnitude greater than that of the slow reactions.

The time dependent enzyme binding model is capable of modeling the results of an ITC experiment. It has already been shown that the algorithm for determining the binding parameters from ITC data can be replicated. The enzyme binding model allows the process to work backwards, given the enzyme binding parameters, the actions of the reaction can be emulated so as to create the binding isotherm calculated from ITC data. The results of this process are shown in Figure 24 and are strikingly similar to the corresponding ITC data from previous work.
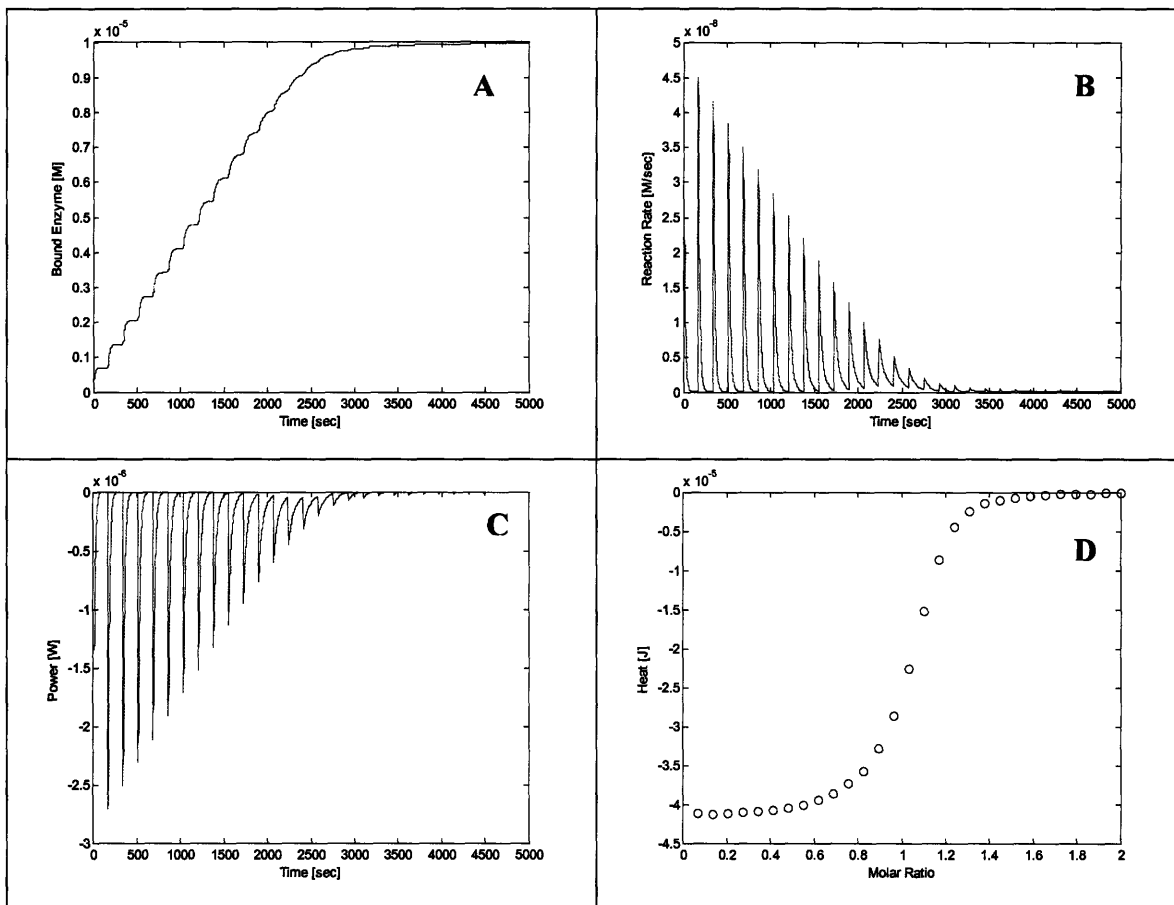
Figure 24: Time dependent enzyme binding response to multiple ligand injectios. A) The concentration of bound enzyme as a function of time. B) The rate of change of the bound enzyme concentration. C) The power output for the system. D) The binding isotherm for the titration.

A new method for measuring binding properties that has been introduced by the MicroCal™ Company is the Single Injection Method for ITC. In this process, the titrant is continuously injected into the analyte inside the reaction cell. The continuous titration method is intended to be a less time consuming method for extracting binding parameters with accuracy that "is comparable to those [thermodynamic parameters] generated by the traditional multiple titration ITC."[1] MicroCal™ includes the results of two comparisons between the multiple and single injection titration methods. These tables are shown in Figure 25.

---

[1] This quotation was found on the MicroCal™ website, http://www.microcal.com/index.php?id=350

Injection Method	Temperature (°C)	Number of experiments	Experiment Time (min)[a]	Stoichiometry (n)	K_B (M^{-1})	ΔH (kcal mol^{-1})
Multiple	15	3	115	0.97 ± 0.02	$(74.6 \pm 7.7) \times 10^6$	-11.1 ± 0.1
SIM	15	4	65	0.98 ± 0.01	$(85.4 \pm 2.0) \times 10^6$	-11.3 ± 0.2
Multiple	35	3	115	0.96 ± 0.02	$(34.9 \pm 7.4) \times 10^6$	-13.1 ± 0.5
SIM	35	4	65	0.96 ± 0.03	$(22.3 \pm 0.9) \times 10^6$	-11.6 ± 0.4

Injection Method	Temperature (°C)	Number of experiments	Experiment Time (min)[a]	Stoichiometry (n)	K_b (M^{-1})	ΔH (kcal mol^{-1})
Multiple	15	1	153.5	1.07	9.03×10^3	-7.63
SIM	15	2	65	1.02 ± 0.01	$(8.01 \pm 0.60) \times 10^3$	-7.69 ± 0.1
Multiple	25	1	153.5	1.01	5.63×10^3	-7.15
SIM	25	2	65	1.04 ± 0.01	$(5.41 \pm 0.21) \times 10^3$	-7.38 ± 0.01
Multiple	40	2	153.5	0.94 ± 0.03	$(3.17 \pm 0.20) \times 10^3$	-7.03 ± 0.26
SIM	40	2	65	1.02 ± 0.01	$(3.49 \pm 0.10) \times 10^3$	-6.69 ± 0.22

[a] Time includes 45 minutes for experimental set-up (cell/syringe washing, cell/syringe filling and cell equilibration)

Figure 25: Data from MicroCal™ website comparing the results of the single injection isothermal titration method to the traditional multiples injection method. The first table is from the titration of Acetazolamide into Carbonic Anhydrase and the second table is from the titration of barium chloride into 18-crown-6. The injections consist of a 100 μL

The precision of repeated SIM measurements (average uncertainty 2.5%) is less than that of the multiple injection method (average uncertainty 5.95%). However, in the data from the Acetazolamide/Carbonic Anhydrase titrations, none of the binding constants for the SIM injections lay within the confidence interval of the multiple injection values or visa versa. Similarly, in the barium chloride/18-crown-6 titrations none of the stoichiometric constants, binding constants, or molar enthalpies of reaction are within the confidence intervals of each other. Figure 26 is an image from the MicroCal™ website that depicts the raw data and binding isotherm for the Acetazolamide/Carbonic Anhydrase SIM titrations. The power data shown in the figure appears have a relatively large noise signal embedded in it with a frequency on the order of 0.01 Hz. This low frequency noise is likely due to the tendency of the ITC power compensation system to overshoot the baseline system temperature. A similar phenomenon was observed in the analysis of the ITC data in Figure 21.
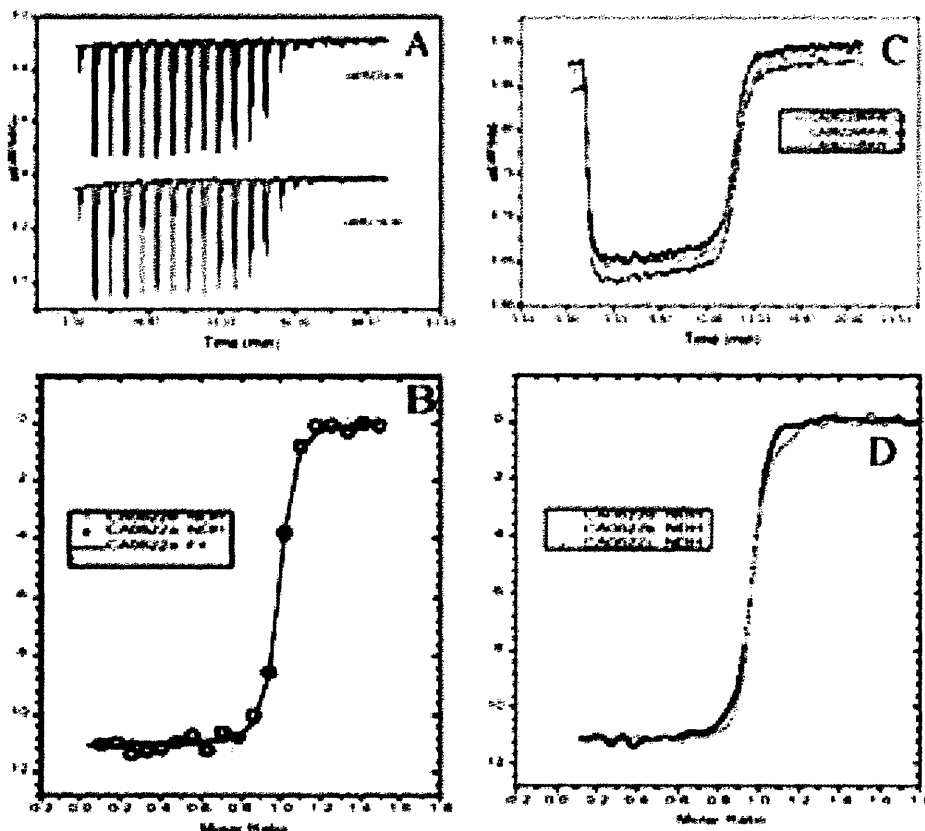
Figure 26: The titration of of Acetazolamide into Carbonic Anhydrase. A) The power output data for two multiple injection experiments. One is shifted on the y-axis for visual clarity. B) The binding isotherm generated from the multiple injection data. C) The power output data for three SIM titrations. D) The binding isotherm generated from the SIM data. Images of multiple injection and SIM data taken from the MicroCal™ website.

Despite the noisy signal, the SIM data still produced more consistent results than the multiple injection method. In the multiple injection method, the function fitting algorithm is limited to a number of data points equal to the number of injections into the analyte. In Figure 26c these 20 discrete data points are visibly fluctuate around the fitted model. In the SIM model, each data point from the power output can be incorporated into the curve fitting model. Integrating the power output over a series of intervals whose minimum size is limited only by the period of the sampling rate, yields the heat produced during that time period. The rate of titrant injection is used to calculate molar ratio of reactants at the time of the integrated heat pulse and these points are used to construct the binding isotherm and determine an optimized set of binding parameters.

The transient model for the enzyme binding reaction can be used to model the SIM process. In the model, the same Acetazolamide/Carbonic Anhydrase system that was previously examined (not to be confused with the recently discussed SIM data) was employed to model the injection of 1.42×10^{-3} moles of ligand over the course of 4000 seconds. The output is shown in Figure 27.
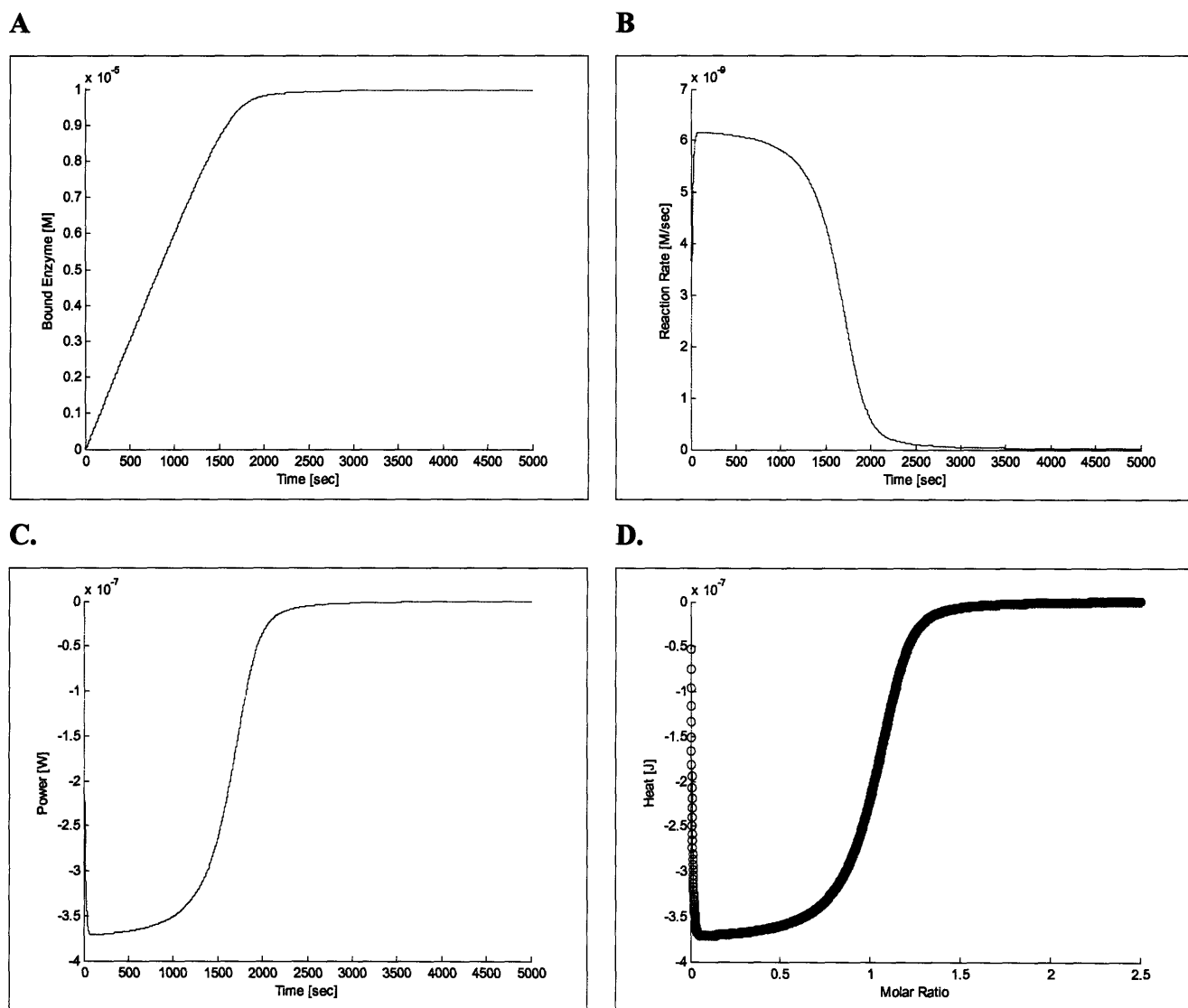

Figure 27: Time dependent enzyme binding response to a continuous ligand injection. A) The concentration of bound enzyme as a function of time. B) The rate of change of the bound enzyme concentration. C) The power output for the system. D) The binding isotherm for the SIM titration.

Conclusion

The investigations with the isoperibol calorimeter have served as an introduction to the complex issues of determining thermal inputs and modeling kinetic properties. The ability to model these very complex systems allows an instrument to be defined and applicable to a variety of different inputs. As work continues in developing a nano-calorimeter instrument there are two important considerations. The first is the challenge and importance of very precisely characterizing and calibrating the thermal response of the system. Without confidence in the behavior of the system no reliable conclusions could be drawn from any data. This issue was a particular problem in this study where the calibration of the system was only a very simplified approximation.

The second consideration is the opportunity to capitalize of the single injection ITC method. SIM measurements are cable of producing significantly more data in a shorter time span than the multiple injection method. In a nanocalorimeter where reactant concentrations are to be minimized, the need to produce very accurate data in the shortest amount of time is paramount.

A final consideration that was investigated in this study was the effect of mixing which was shown to increase the response time of the system. Mixing was also shown to add energy and noise into the system. In a precise nano-calorimeter the disadvantages of this high frequency noise and offset may outweigh the benefits of mixing especially since the thermal and mass transport obstacles will be reduced given the smaller length scale.

Acknowledgements

References

1. Lama, R. F., Lu, C. Y., "Excess Thermodynamic Properties of Aqueous Alcohol Solutions," *J. Chem. Thermodyn. Data*, 1965 (10), 216-219.
2. Clever, H.L., Pigott, S. P., "Enthalpies of Mixing of Dimethylsulfoxide with Water and with Several Ketones at 298.15 K," *J. Chem. Thermodyn.*, 1971 (3), 221-225.
3. Chatterfee, N. D., Fluc, S. "Thermodynamic Mixing Properties of Muscovite-Paragonite Crystalline Solutions at High Temperatures and Pressures, and their Geological Applications" *J. Petrology*. 1986 (27), 677-693.
4. Ladbury, J. E., Chowdhry, B. Z., "Sensing the heat: the application of isothermal titration calorimetry to the thermodynamic studies of biomolecular interactions" *Chemistry & Biology*, 1996 (3), 10, 791-801.
5. Ladbury, J. E., Doyle, M. L., Eds, *Biocalorimetry 2: Applications of Calorimetry in the Biological Sciences*, 2004
6. Grime, K. J., Eds *Analytical Solution Calorimetry;*. ISSN 0069-2883, John Wiley & Sons Inc. 1985; Vol. 79
7. Wiseman, T., Williston, S., Brandts, J.F., Lin, L.-N., "Rapid measurement of binding constants and heats of binding using a new titration calorimeter" *Anal. Biochem.*, 1989 (179), 131-137.
8. Plesner, I. W., Bülow, A., Bols, M. "Accurate determination of rate constants of very slow, tight-binding competitive inhibitors by numerical solution of differential equations, independently of precise knowledge of concentration" *Anal. Biochem.*, 2001 (295), 183-193.
9. Ladbury, J. E., Chowdhry, B. Z., Eds. *Biocalorimetry: Applications of Calorimetry in the Biological Sciences*, ISBN 0-471-97781-0, John Wiley & Sons, West Sussex, England
10. Sigurskjold, B.WExact analysis of competition ligand binding by displacement isothermal titration calorimetry. *Anal. Biochem.* 2000 (277), 260-266.